AJNR

This information is current as of April 20, 2026.

Volumetric Postcontrast T1 Turbo Spin-Echo versus Gradient-Recalled Echo MR sequences for Detecting Brain Metastases: a Systematic Review and Meta-analysis

Anass Benomar, Sukhmanjit S. Ghumman, Youcef Ouahdi, Sherief Ghozy, Hany Soliman, Kang Liang Zeng, Chia-Lin Tseng, Jay Detsky, Hanbo Chen, Deepak Dinakaran, Qing Fu, Sean Symons, Arjun Sahgal, Chris Heyn and Pejman Jabehdar Maralani

AJNR Am J Neuroradiol published online 12 March 2026
http://www.ajnr.org/content/early/2026/03/12/ajnr.A9294

Published March 12, 2026 as 10.3174/ajnr.A9294

Volumetric Postcontrast T1 Turbo Spin-Echo versus Gradient-Recalled Echo MR sequences for Detecting Brain Metastases: a Systematic Review and Meta-analysis

Anass Benomar, Sukhmanjit S. Ghumman, Youcef Ouahdi, Sherief Ghozy, Hany Soliman, Kang Liang Zeng, Chia-Lin Tseng, Jay Detsky, Hanbo Chen, Deepak Dinakaran, Qing Fu, Sean Symons, Arjun Sahgal, Chris Heyn, and Pejman Jabehdar Maralani

ACCEPTED MANUSCRIPT

ABSTRACT

BACKGROUND: Contrast-enhanced 3D T1-weighted MRI is the imaging reference for detection and follow-up of brain metastases. Volumetric GRE-based sequences, such as MPRAGE, are widely used but remain prone to susceptibility and lower lesion conspicuity. 3D black-blood TSE-based sequences, such as Sampling Perfection with Application-Optimized Contrasts by using different flip angle Evolutions (SPACE), have been increasingly embedded into routine workflow and are thought to improve lesion detection in part through vessel signal suppression.

PURPOSE: We aimed to investigate the comparative diagnostic performance of 3D T1 TSE versus GRE sequences for the detection of brain metastases.

DATA SOURCES: Studies comparing the diagnostic performance of postcontrast 3D T1 SE and GRE sequences in adults with brain metastases were searched on MEDLINE, EMBASE, Cochrane Central, Google Scholar, and PROSPERO, from inception through April 2025.

STUDY SELECTION: Fifteen studies encompassing 544 patients with 4338 metastases were included.

DATA ANALYSIS: Data on diagnostic accuracy parameters, image quality, and inter-rater agreement were extracted. Random-effects models were applied to compute pooled sensitivity and comparative OR for lesion detection. Risk of bias was assessed using QUADAS-2 and QUADAS-C tools.

DATA SYNTHESIS: Pooled sensitivities for detection of brain metastases were 97.4% (95%CI, 93.2%-99.0%) for TSE and 76.1% (95%CI, 69.3-81.9) for GRE-based sequences, with a comparative OR of 12.0 (95%CI, 5.45-26.6, P <.0001). Detectability of small lesions (<5 mm) was significantly better on TSE (96.1%; 95%CI, 87.7-98.8) than GRE (58.4%; 95%CI, 47.9-68.2), while both techniques performed comparably for larger (≥5 mm) lesions (98.2% for TSE, 94.4% for GRE). OR estimates were 17.2 (95%CI, 4.50-66.1) for small and 2.81 (95%CI, 0.92-8.56) for large lesions. Contrast-to-noise-ratio and inter-rater agreements were slightly higher on TSE than GRE. False positives were more common with TSE, mostly related to incomplete vessel suppression (49 FP counts in TSE, 35 in GRE).

LIMITATIONS: Our meta-analysis is limited by high heterogeneity, case-only studies, possible small-study effects, and high risk of bias for the reference standard domain.

CONCLUSIONS: Postcontrast 3D T1 TSE sequences provide higher sensitivity and improved lesion conspicuity compared with GRE sequence, particularly for small metastases, though at the cost of slightly higher false positives.

ABBREVIATION: CNR = Contrast-to-noise-ratio; DANTE = Delay Alternating with Nutation for Tailored Excitation; FN = False Negatives; FP = False Positives; MSDE = Motion-Sensitized Driven-Equilibrium; SPACE = Sampling Perfection with Application-Optimized Contrasts by using different flip angle Evolutions; SRS = Stereotactic Radiosurgery; TP = True Positives; VISTA = Volume ISotropic Turbo spin-echo Acquisition

INTRODUCTION

Contrast-enhanced T1-weighted MRI is considered the reference standard for detecting and monitoring brain metastases, with several sequence types available in routine clinical practice. Three-dimensional T1-weighted GRE sequences, such as FLASH and MPRAGE, have long been widely used because they provide high-resolution reformattable imaging with relatively short acquisition times.[1] However, lesion conspicuity on GRE-based sequences

Received January 8, 2026; accepted after revision March 9.

From the Department of Medical Imaging (A.B., S.S., C.H., P.J.M.), Radiation Oncology (H.S., K.L.Z., C.-L.T., J.D., H.C., D.D.,A.S.), Sunnybrook Health Sciences Centre, University of Toronto, Toronto, ON, Canada; Department of Radiology (S. S.G.), Jewish General Hospital, McGill University Health Centre, Montreal, QC, Canada; Faculty of Medicine (Y.O.), University of Montreal, Montreal, QC, Canada; Departments of Radiology and Neurologic Surgery (S.G.), Mayo Clinic, Rochester, MN, USA and Department of Radiology (Q.F.), Union Hospital, Tongji Medical College, Huazhong University of Science and Technology, Wuhan, China.

Corresponding Author: Dr. Anass Benomar, MD MSc, Department of Medical Imaging, Division of Neuroradiology, Sunnybrook Health Sciences Centre, University of Toronto, 2075 Bayview Avenue, Toronto, ON, Canada M4N 3M5; e-mail: anass.benomar@umontreal.ca

http://dx.doi.org/10.3174/ajnr.A9294

Copyright 2026 by American Society of Neuroradiology.

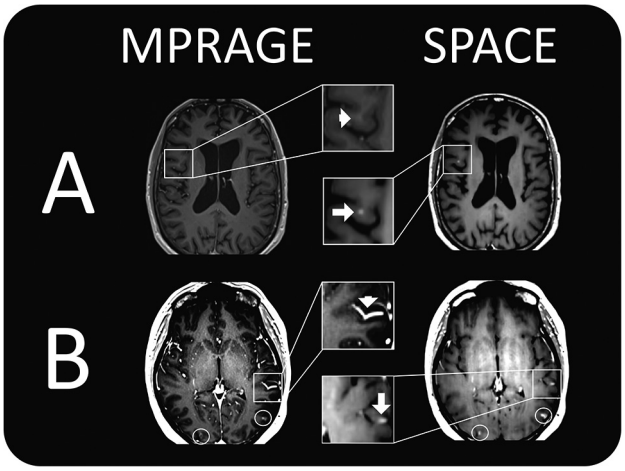


FIG 1. Comparison of contrast-enhanced 3D T1-weighted GRE (MPRAGE) and 3D T1-weighted TSE (SPACE) sequences in two patients with known metastatic brain disease. In patient **A**, SPACE demonstrates a distinct focal enhancing lesion in the right frontal operculum that is highly suspicious for metastasis (*arrow*) but remains inconspicuous on the corresponding MPRAGE image (*arrowhead*). In patient **B**, SPACE shows a focus of enhancement in the left temporal lobe which could be mistaken for a metastatic lesion (*arrow*), whereas the corresponding MPRAGE image reveals clear linear enhancement consistent with a vessel (*arrowhead*). SPACE also delineated metastatic lesions more conspicuously compared to MPRAGE (*circles*). Except the left temporal vascular enhancement in patient **B**, all the remaining suspicious enhancing foci in patients **A** and **B** have increased in size on follow-up scans and were thus considered metastatic lesions.

may be limited by prominent signal from cortical and pial vessels and relatively high background signal within normal white matter, which can obscure small enhancing lesions. Historically, volumetric T1-weighted TSE sequences were constrained by prolonged acquisition times and low SNR (especially at 1.5T for the latter).[2] Advances related to variable flip angle techniques have enabled the development of clinically viable 3D T1 TSE sequences, such as Sampling Perfection with Application-Optimized Contrasts by using different flip angle Evolutions (SPACE, Siemens), CUBE (GE) or Volume ISotropic Turbo spin-echo Acquisition (VISTA, Philips). These sequences provide effective vascular signal suppression ("black-blood" effect) and lower background parenchymal signal, thereby improving the conspicuity of enhancing lesions (**Fig 1**).[3–6]

A meta-analysis published in 2016 by Suh et al. reported higher pooled sensitivity with 3D T1 TSE sequences compared GRE sequences for the detection of brain metastases, particularly for lesions 5 mm or smaller.[7] However, the analysis focused exclusively on lesion detection and did not assess false positive (FP) findings. This limitation is clinically relevant, as incomplete vascular suppression may generate pseudo-enhancing foci and overestimate intracranial disease burden.

In parallel, the management of brain metastases has undergone a major paradigm shift. Stereotactic radiosurgery (SRS), once restricted to patients with a limited number of lesions, is now increasingly applied to patients with multiple metastases, driven by improved systemic disease control, more favorable neurocognitive outcomes compared with whole-brain radiotherapy, and advances in imaging.[8–10] In this context, where treatment decisions are highly dependent on accurate lesion count and localization, an updated synthesis of the diagnostic performance of 3D T1 TSE and GRE sequences is warranted.

We conducted a systematic review and meta-analysis of studies comparing the diagnostic performance of contrast-enhanced 3D T1-weighted TSE and GRE sequences for the detection of brain metastases. Our primary objectives were to compare sensitivity, detection OR, and FP findings between the two sequence types. A secondary objective was to assess reported image quality metrics, including contrast-to-noise ratio (CNR).

MATERIALS AND METHODS

This study was conducted in accordance with the Preferred Reporting Items for Systematic Reviews and Meta-Analyses (PRISMA) guidelines.[11] The study protocol was not prospectively registered.

Search Strategy

A systematic literature search was conducted on MEDLINE, EMBASE, Cochrane Central Register of Controlled Trials, and Google Scholar to identify original articles reporting the comparative detection of brain metastases in 3D T1 TSE and GRE sequences, from inception up to April 11, 2025, by two institutional librarians. PROSPERO registry was additionally queried to identify ongoing or unpublished systematic reviews. The search strategy was independently peer-reviewed and is further detailed in the **Supplemental Data**.

Eligibility Criteria

Original research studies with 1) adult patients, 2) known for primary extracranial neoplasm with brain metastases, 3) who have undergone an MRI brain with both contrast-enhanced 3D T1 TSE and GRE sequences, and for whom the detection rate and MR image quality (such as CNR) were reported for both sequences, were included.

Studies were excluded if they were published in a language other than French, English, or Spanish; were reviews, case reports, editorials, or conference abstracts; included fewer than 10 metastases in total; involved primary CNS neoplasms or other coexisting CNS pathologies; lacked sufficient data to compute detection rates; evaluated non-volumetric (2D) sequences only; or did not directly compare 3D T1 TSE and GRE sequences.

Screening Process and Data Extraction

Covidence systematic review software (Veritas Health Innovation, Melbourne, Australia. www.covidence.org) was used for all screening stages and initial data extraction. Title/abstract and full-text screening were independently performed by three authors (A.B., S.S.G., Y.O.). Data extraction was performed by two authors (A.B. and S.S.G.), with discrepancies resolved by consensus. Reference lists of included studies and prior meta-analyses were screened to ensure completeness.

The following data were collected from included studies: first author, year of publication, country, total number of patients, total number of brain metastases, method to establish ground truth (reference standard), MRI field strength and vendor, age, sex, site of primary neoplasms, 3D T1 TSE and GRE reported

ACCEPTED MANUSCRIPT

names and sequence order, voxel size, IV contrast name and dose, diagnostic accuracy parameters for each sequences (true positives (TP), FP, false negatives (FN), true negatives, sensitivity, specificity), the reason for false positives, CNR (lesion-background), the number of readers and agreement coefficient estimates. When not explicitly reported in the study, missing diagnostic accuracy values were obtained by contacting study authors or, whenever feasible, manually estimated using available data. In reader studies, consensus readings were used to populate the 2x2 diagnostic contingency table. If no consensus readings were reported, results from the observer having the highest detection rate were extracted.

Risk of Bias Assessment

The risk of bias was evaluated using QUADAS-2 and QUADAS-C tools.[12,13] These complementary tools assess bias across four domains: patient selection, index test, reference standard, and flow and timing.

Statistical Analyses

Statistical analyses were performed using R version 4.5.1 (R Foundation for Statistical Computing, Vienna, Austria, http://www.r-project.org/). Sensitivity for each sequence was calculated from reported TP and FN counts with 95% CI. Comparative performance was summarized as an OR of lesion detection (3D T1 TSE vs GRE), based on the TP-to-FN ratio for each sequence.[14] This conditional detection OR reflects comparative sensitivity among diseased-only cases and should not be mistaken for the more frequently used diagnostic OR **(Supplemental Data)**. Pooled estimates of sensitivities and log-transformed ORs were obtained using a random-effects inverse-variance model with between-study variance estimated by restricted maximum likelihood and Hartung–Knapp adjustment.[15] When TP or FN values equaled zero, a continuity correction of 0.5 was used. Heterogeneity was assessed using Cochran's Q and I^2. Because discordant-pair information was inconsistently reported, paired McNemar analyses were not feasible. Publication bias was estimated using Egger's regression test for funnel plot asymmetry, with $P < .10$ considered significant.[16] Subgroup analyses were performed by lesion size according to reported cut-offs. Outlier studies were identified using visual inspection, 'leave-one-out' method, and the "outlier and influence diagnostics" methods as reported by Viechtbauer and Cheung.[17]

RESULTS

Search and Screening Results

After duplicate removal, 2808 records were identified; 2768 were excluded after title and abstract screening and 25 after full-text review, yielding 15 included studies (**Fig 2**).

Design of Included Studies

Most included studies were retrospective, reader-based, case-only, comparative diagnostic accuracy studies comparing at least one TSE-based and one GRE-based postcontrast 3D T1 sequences in terms of detectability of brain metastases. 5 studies (33%) were prospective. Only two studies included healthy controls for full diagnostic accuracy purposes.[18,19] Four studies additionally evaluated other 2D or 3D MR sequences beyond the primary volumetric TSE- and GRE-based acquisitions.[5,18,20,21]

Patient Characteristics

Detailed patient and imaging characteristics of the included studies are available in the **Supplemental Data**. A total of 544 patients with 4338 brain metastases were included. Mean age across studies was 60.7± 3.3 years (range of reported means, 55.0-64.9 years). 44% (240/544) of patients were females. The total number of metastases per included study (regardless of the number of patients) varied between 11 and 832. Lung cancer was the most frequent primary (65%, 351/544), followed by breast (15%) and melanoma (6%). Leptomeningeal and dural metastases were excluded from all studies.

MR Imaging Characteristics

All studies except one were performed on 3T MRI scanners.[22] Across studies, Postcontrast 3D T1 TSE-based sequences were most often SPACE or equivalent black-blood TSE variants, whereas 3D T1 GRE-based sequences were predominantly MPRAGE, with a few alternative vendor-specific implementations (**Supplemental Data**). TSE techniques were enhanced with Motion-Sensitized Driven-Equilibrium (MSDE) in 5 studies, and with Delay Alternating with Nutation for Tailored Excitation (DANTE) in 2 studies, to achieve higher vessel signal suppression. In most studies, both TSE and GRE sequences were using 1 mm^3 (or less) volumetric postcontrast acquisitions covering the whole brain, except for the study of Lee et al. which used a larger voxel size of 2 mm^3.[23] Gd-DTPA and Gadobutrol were the most frequently used contrast agents in 6 (40%) studies each, respectively. Twelve studies (80%) either randomized or alternated the sequence order to avoid bias related to changing concentrations and lesion enhancement with time (**Supplemental Data**). The three remaining studies either started with TSE (2/3) or GRE (1/3) first.

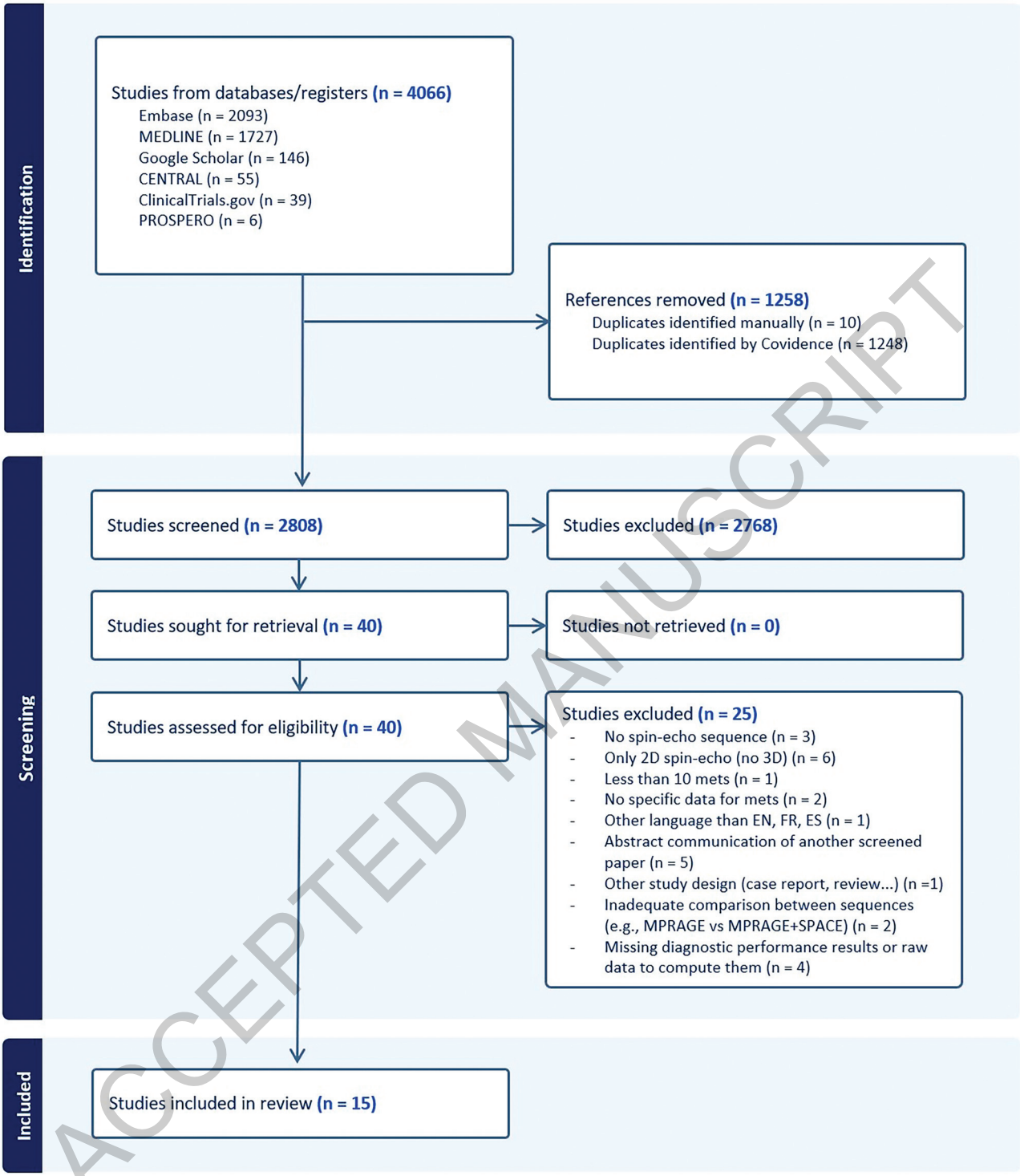
Reference Standard Adjudication

Two studies (13%) mentioned the use of histopathologic diagnosis (in combination with radiological data) for reference standard adjudication of brain metastases, with only one study (Danieli et al.) specifically reporting the number of lesions adjudicated in that manner.[20,24] The remaining studies used radiological criteria alone for establishing the diagnosis. Allowing for wording differences, most studies followed Kato et al. definition of true metastasis: 1) the enhancing lesion is not a normal structure or an artifact; 2) the lesion is located in the brain parenchyma (with typical imaging findings of irregular, circular or nodular enhancement); 3) the size of the lesion either decreased after therapy or increased on follow-up MR images.19 This was either adjudicated by consensus between participating readers (11/15 studies, 73%), or by an independent reader not participating in the core assessment (3/15, 20%). One study did not mention how and who adjudicated the reference standard result.[25]

Inter-Rater Agreement for Lesion Detection

All studies included a multireader assessment, with a majority involving two observers only (13/15, 87%). Agreement between raters for detection of cerebral metastases was separately reported for each MR sequence type in 11 studies (73%), using κ statistics or intraclass coefficients. For TSE-based sequences, inter-rater agreement

ACCEPTED MANUSCRIPT



ACCEPTED MANUSCRIPT

FIG 2. Study flow diagram.

varied between 0.72 and 1.00, and for GRE-based sequences, it varied between 0.65 and 1.00 (Supplemental Data). Only Chen Zhou et al. reported 95% CI with their agreement estimate, precluding further meta-analysis due to the lack of dispersion data.[22]

Image Quality

Of 15 included studies, 9 (60%) reported CNR estimates using various formulas (**Supplemental Data**), contributing to heterogeneity. Given this limitation and the lack of dispersion measures, meta-analysis of CNR estimates was not performed. Reported CNR estimates varied between 1.7 and 89.1 for TSE-based sequences, and between 1.4 to 19.6 for GRE-based sequences, with a trend toward better CNR in TSE-based sequences (**Supplemental Data**). The SNR and qualitative assessments of image quality (e.g., Likert scales) were inconsistently reported across studies and thus not considered for the current study.

Lesion Detectability: Sensitivity

All studies but two were" case-only" by design and only recruited patients with intracranial metastases.[18,19] The absence of healthy controls precludes computation of specificity, FP rates, diagnostic OR and ROC curves.

Across 15 studies, for TSE-based sequences, reported sensitivity ranged from 82.2% to 100%, with a pooled sensitivity estimate of 97.4% (95%CI, 93.2-99.0) (Fig 3). Similar sensitivities were observed with or without vessel signal suppression add-ons (**Supplemental Data**). Sensitivity for GRE-based sequences ranged from 55.3% to 98.1%, with a pooled estimate of 76.1% (95%CI, 69.3-81.9).

7 studies (47%) reported sensitivity stratified by lesion size. One study used a 3 mm cut-off,[21] and the remainder, a 5 mm cut-off (**Supplemental Data**). Lesions were grouped as 'small' (<3 or <5 mm) or 'large' (≥3 or ≥5 mm) as reported. For small lesions, sensitivity varied between 73.1 and 100% for TSE-based sequences, and between 45.9% and 80.0% for GRE-based sequences across studies, with pooled sensitivity estimates of 96.1% (95%CI, 87.7-98.8) and 58.4% (95%CI, 47.9-68.2), respectively. For large lesions, reported sensitivity varied between 94.9% and 100% for TSE-based sequences, and between 85.7% and 100% for GRE-based sequences, with pooled estimates of 98.2% (95%CI, 95.6-99.2) and 94.4% (95%CI, 89.9-97.0), respectively (Fig 4). The small (n=3) number of studies with fixed sequence order precludes further subgroup analyses based on sequence order.

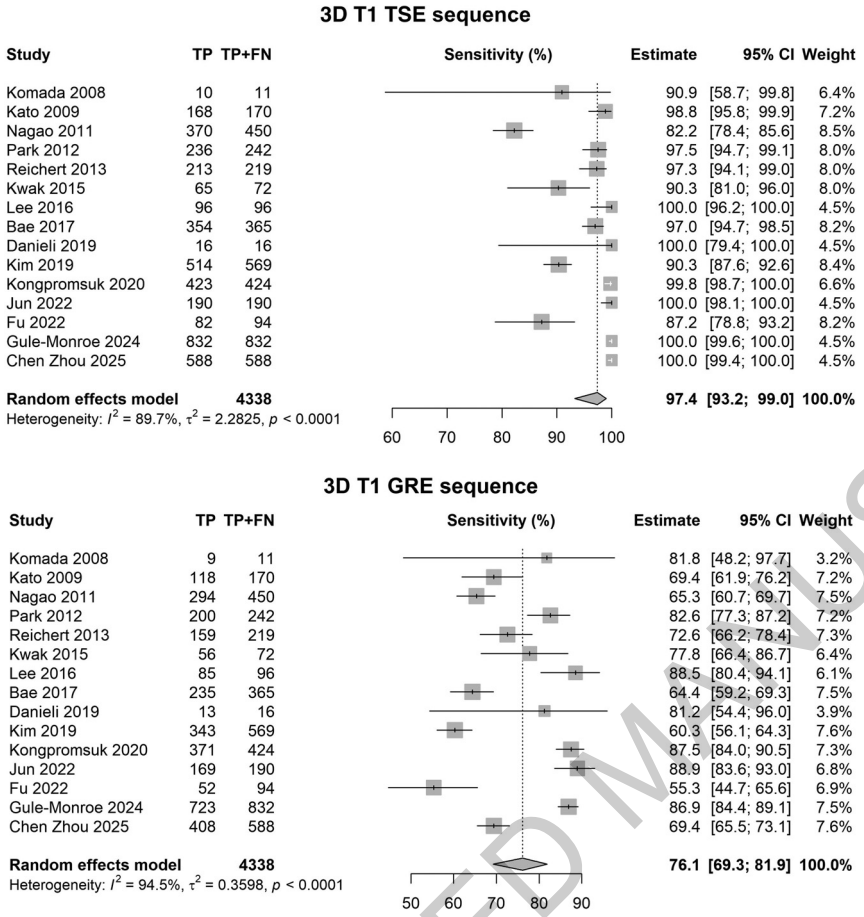


FIG 3. Forest plot of sensitivity estimates for 3D T1 TSE and GRE-based sequences.

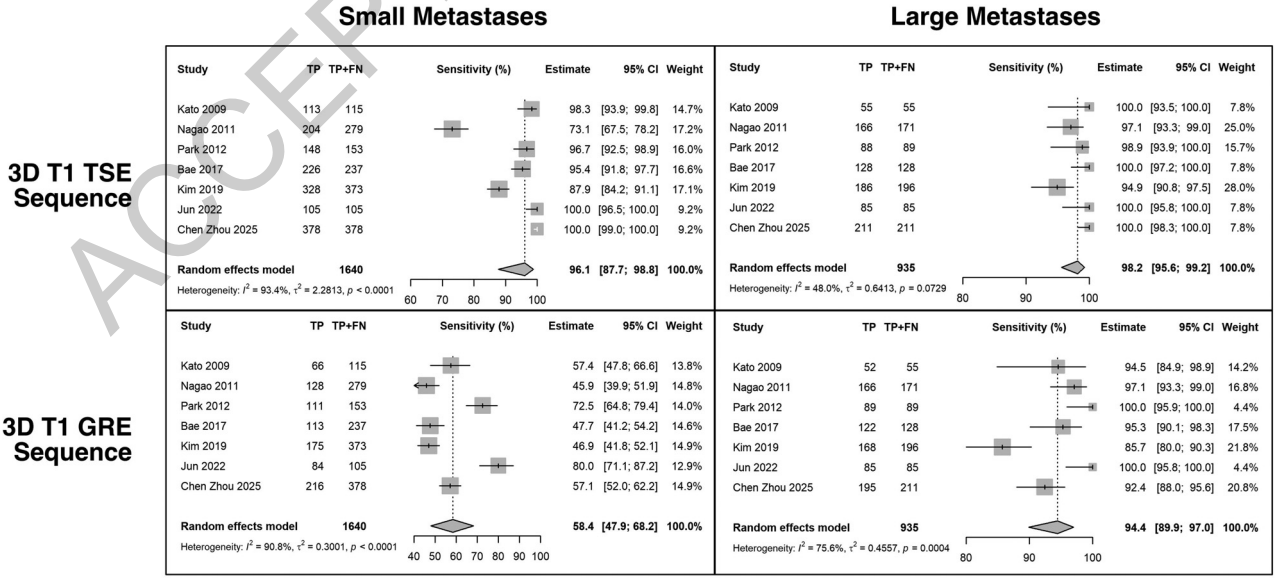


FIG 4. Forest plot of sensitivity estimates for 3D T1 TSE and GRE-based sequences, stratified by lesion size. Across studies, lesion size dichotomization cut-off between small and large lesions was defined as 5 mm in 6 studies, and 3 mm in one study.

ACCEPTED MANUSCRIPT

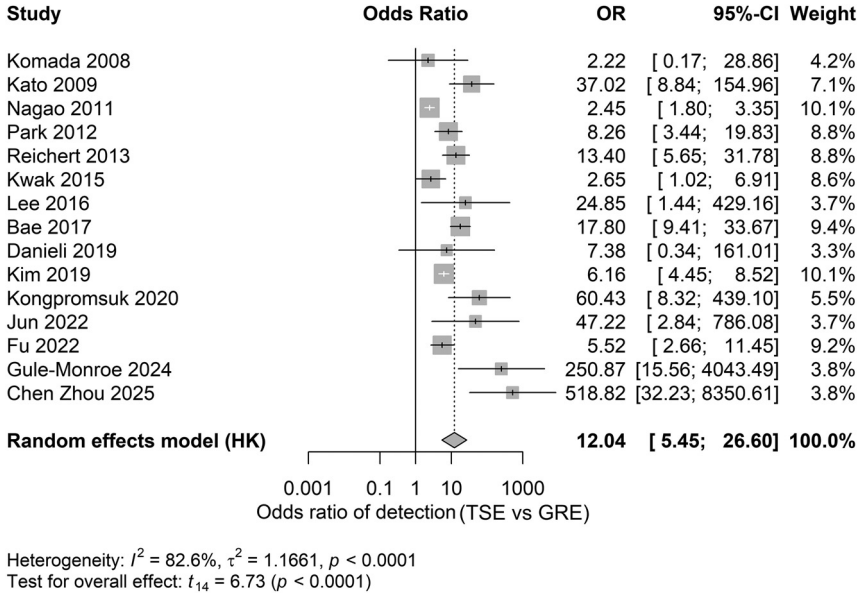


FIG 5. Forest plot of detection OR estimates (TSE vs GRE).

Lesion Detectability: Comparative Odds Ratio

Comparative OR for lesion detection (TSE vs. GRE) varied between 2.22 and 518.8 across studies, with a pooled OR estimate of 12.0 (95%CI, 5.45-26.6; P <.0001), showing superior lesion detection in TSE over GRE-based sequences (Fig 5). In the subgroup analysis restricted to the 7 studies reporting results per lesion size, TSE-based sequences outperformed GRE-based sequences for detecting small lesions (OR=17.2, 95%CI, 4.50-66.1; P = .002), however both sequences performed similarly for large lesions (OR=2.81, 95%CI, 0.92-8.56; P = .063). The test for subgroup differences confirmed a statistically significant interaction between lesion size and sequence performance (χ^2 = 6.47, P = .011), indicating that lesion size significantly affects the relative detection performance of TSE versus GRE (**Supplemental Data**).

Sensitivity Analyses and Influence Diagnostics

Between-study heterogeneity for OR detection meta-analysis was substantial (I^2 = 82.6%; Q = 80.45, df = 14, P < .0001). Stratification by lesion size allowed to decrease heterogeneity only for the large lesion group (I^2 = 27.3%; P < .22). Influence diagnostics identified three outlier studies,[22,25,26] whose exclusion resulted in a modest reduction in heterogeneity (I^2 = 60.0%) while yielding a similar pooled effect (OR = 9.90, 95% CI, 5.50-17.8; P =.0039). Funnel plot asymmetry was suggested by Egger's linear regression test (t = 2.87, df = 13, P = .013), indicating potential small-study effects. Sensitivity and influence analyses of the pooled sensitivity estimates for each sequence yielded similar findings, with high heterogeneity and no dominant influential studies (**Supplemental Data**).

False Positive Counts and Causes

As mentioned above, computation of FP rates was methodologically impossible because of the absence of TN (healthy controls). However, given their importance for our research topic, we chose to explore reported FP for descriptive purposes. 12 studies (80%) specifically reported FP counts and reasons behind these (**Supplemental Data**). Across studies, FP on TSE-based sequences were mainly due to incomplete suppression of slow venous flow, producing enhancement in sinuses or deep venous structures, and occasionally in choroid plexus or meninges. In contrast, GRE-based sequences predominantly generated FP from intensely enhancing superficial cortical or pial vessels, sometimes accentuated by flow-related pulsation and partial-volume artifacts. Enhancing subacute infarction was also noted for GRE in one study. Per study, FP counts ranged from 0 to 18 for TSE-based sequences, and from 0 to 17 for GRE-based sequences, with an overall higher cumulative FP count of 49 (for TSE) compared to 35 (for GRE).

Risk of Bias and Applicability Concerns

A systematically higher risk of bias was found in the reference standard domain, as 10 out of 15 studies defined Reference Standard adjudications using either or both MR sequences (index tests), and all were based on reader adjudication, subject to variability. Six studies (40%) demonstrated unclear or high risk of bias for the Patient Selection domain due to nonconsecutive sampling (or lack of details regarding selection), and 3 studies were at risk of bias for the Flow and Timing domain because of fixed or unequal order of 3D T1 TSE and GRE sequence acquisitions. Predominantly low concerns for applicability were found across all domains (**Supplemental Data**).

DISCUSSION

In this systematic review and meta-analysis of 15 studies yielding 544 patients and 4338 brain metastases, contrast-enhanced 3D T1-weighted TSE sequences demonstrated higher sensitivity for lesion detection than 3D T1 GRE sequences, with pooled sensitivities of 97.4% and 76.1% respectively, and a pooled detection OR of 12.0 (**Figs 3 and 5**). This advantage was most pronounced for small metastases (< 5 mm), whereas both methods performed similarly for larger lesions. Reported CNR values and inter-rater agreement estimates also favored TSE over GRE-based sequences. This observed superiority is likely multifactorial and driven by several key physical and contrast mechanisms, including (but not limited to): stronger magnetization transfer effects resulting in decreased white matter signal, elimination of T2* effects due to 180-degree refocusing pulses, effective vessel signal suppression, and greater sensitivity to contrast enhancement.[20,27,28]

These findings expand upon the prior meta-analysis of Suh et al.,[7] which synthesized 8 early 3T studies (252 patients, 1413 lesions) and demonstrated superior detectability for 3D T1 TSE techniques, particularly for small metastases. The present analysis adds nearly a decade of data, including newer black-blood variants (with DANTE or iMSDE add-ons) and higher-channel head coils, confirming that TSE-based sequences maintain a diagnostic

ACCEPTED MANUSCRIPT

edge even with optimized GRE conditions. Moreover, our inclusion of FP data provides a more balanced appraisal of clinical trade-offs. Although vascular signal suppression improves lesion detection and contrast on TSE-based sequences, a higher number of FP was observed, primarily related to incomplete suppression of slow venous flow.

The increasing use of SRS for patients with multiple brain metastases underscores the importance of precise lesion detection and enumeration. Underestimation of small metastases may directly influence treatment eligibility, target volume definition, and follow-up strategy.[8] TSE-based techniques offer higher lesion-to-parenchyma contrast and more homogeneous enhancement, which may facilitate target delineation for SRS planning and potentially improve patient outcomes.[10,29] While GRE-based sequences remain adequate for larger lesions, their reduced sensitivity for small metastases suggests that reliance on GRE alone may underestimate intracranial disease burden. Conversely, using TSE-based sequence alone for detection of brain metastases might increase the likelihood of radiating small vessels misdiagnosed as lesions, an undesirable outcome. From a practical standpoint, several factors influence implementation beyond diagnostic performance alone. Greater radiologist familiarity with MPRAGE (and equivalents), along with faster acquisition times and cross-vendor standardization, contrasts with the more heterogeneous and vendor-specific implementations of TSE-based sequences, which may limit their adoption as a standalone replacement. A combined TSE and GRE imaging approach may represent a pragmatic compromise to maximize sensitivity while mitigating FP findings, albeit at the cost of modestly increasing acquisition time. Recent studies evaluating combined approaches have reported higher sensitivity than GRE alone[10] and fewer FP compared with TSE alone,[30] although differences were not always statistically significant.

An important methodological consideration relates to the imperfect reference standards used across studies, which predominantly relied on radiologic assessment and longitudinal follow-up rather than histopathologic confirmation. Furthermore, many studies incorporated one or both index MR sequences into reference standard adjudication, introducing potential incorporation bias that might have inflated sensitivity estimates. An additional layer of variability is also introduced by reader adjudication of the reference standard, rather than a more objective way to establish ground truth. This important limitation cannot however be overcome and can thus only be acknowledged, as most small or multiple metastases are not surgically sampled, and histology cannot feasibly serve as a universal gold standard in this clinical context.

This work has several limitations. First, most included studies were retrospective and case-only by design, precluding estimation of specificity and formal FP rates. The pooled conditional detection OR estimates should only be interpreted as measures of comparative sensitivity among patients with brain metastases rather than comprehensive diagnostic accuracy, particularly when extrapolating to surveillance or screening contexts. Second, substantial between-study heterogeneity was present despite stratification by lesion size, likely reflecting differences in MR scanners and coils, patient selection, and reference standard adjudications. Third, our results are not applicable to extra-axial metastases as these were excluded from all studies. Fourth, although 3D T1-weighted TSE sequences are now known to be technically feasible at both 1.5T and 3T, only 1 included study was performed at 1.5T, limiting the generalizability of our results to centers without routine access to 3T MRI. Further comparative studies using 1.5T MR magnets might be required. Fifth, all included studies involved human readers only. Whether our results would be similar if studies using machine- or deep-learning algorithms were included remains yet to be explored. Finally, studies evaluating single-sequence diagnostic accuracy or combined-sequence protocols were excluded for methodological reasons, and the present findings should not be extrapolated to those settings.

CONCLUSIONS

3D T1 TSE-based sequences are more sensitive than 3D T1 GRE-based sequences in detecting brain metastases, especially for smaller lesions, but are associated with more FP. Meta-analyses assessing the detectability of brain metastases using combined SE and GRE sequences should be explored.

ACCEPTED MANUSCRIPT

ACKNOWLEDGMENTS

The authors would like to thank Ms. Emma Wilson, MLIS, BHSc, and Ms. Catherine Devion, MLS (Library Services, Sunnybrook Health Sciences Centre) for their methodological expertise and support in developing the systematic search strategy.

Disclosure forms provided by the authors are available with the full text and PDF of this article at www.ajnr.org.

REFERENCES

1. Chappell PM, Pelc NJ, Foo TK, et al. **Comparison of lesion enhancement on spin-echo and gradient-echo images.** *AJNR Am J Neuroradiol.* 1994;15:37–44 Medline
2. Mugler JP, 3rd, Bao S, Mulkern RV, et al. **Optimized single-slab three-dimensional spin-echo MR imaging of the brain.** *Radiology.* 2000;216:891–899 CrossRef Medline
3. Park J, Kim J, Yoo E, et al. **Detection of small metastatic brain tumors: Comparison of 3D contrast-enhanced whole-brain black-blood imaging and MP-RAGE imaging.** *Investigative Radiology.* 2012;47:136EP–141 CrossRef Medline
4. Yuan J, Law SCK, Wong KK, et al. **3D T1-weighted turbo spin echo contrast-enhanced MRI at 1.5 T for frameless brain metastases radiotherapy.** *J Cancer Res Clin Oncol.* 2022;148:1749–1759 CrossRef Medline
5. Fu Q, Cheng QG, Kong XC, et al. **Comparison of contrast-enhanced T1-weighted imaging using DANTE-SPACE, PETRA, and MPRAGE: A clinical evaluation of brain tumors at 3 Tesla.** *Quantitative Imaging in Medicine and Surgery.* 2022;12:592EP–607 CrossRef Medline
6. Kwak HS, Hwang S, Chung GH, et al. **Detection of small brain metastases at 3 T: Comparing the diagnostic performances of contrast-enhanced T1-weighted SPACE, MPRAGE, and 2D FLASH imaging.** *Clinical Imaging.* 2015;39:571EP–575 CrossRef Medline
7. Suh CH, Jung SC, Kim KW, et al. **The detectability of brain metastases using contrast-enhanced spin-echo or gradient-echo images: a systematic review and meta-analysis.** *J Neurooncol.* 2016;129:363–371 CrossRef Medline

8. O'Beirn M, Benghiat H, Meade S, et al. **The Expanding Role of Radiosurgery for Brain Metastases.** *Medicines (Basel)*. 2018;5 CrossRef Medline
9. Welzel T, El Shafie RA,Nettelbladt VB, et al. **Stereotactic radiotherapy of brain metastases: clinical impact of three-dimensional SPACE imaging for 3T-MRI-based treatment planning.** *Strahlentherapie und Onkologie*. 2022;198:926EP–933 CrossRef Medline
10. Kutuk T, Abrams KJ, Tom MC, et al. **Dedicated isotropic 3-D T1 SPACE sequence imaging for radiosurgery planning improves brain metastases detection and reduces the risk of intracranial relapse.** *Radiotherapy and Oncology*. 2022;173:84EP–92 CrossRef Medline
11. Page MJ, McKenzie JE, Bossuyt PM, et al. **The PRISMA 2020 statement: an updated guideline for reporting systematic reviews.** *BMJ*. 2021;372:n71 CrossRef Medline
12. Whiting PF, Rutjes AW, Westwood ME, et al. **QUADAS-2: a revised tool for the quality assessment of diagnostic accuracy studies.** *Ann Intern Med*. 2011;155:529–536 CrossRef Medline
13. Yang B, Mallett S, Takwoingi Y, et al. **QUADAS-C: A Tool for Assessing Risk of Bias in Comparative Diagnostic Accuracy Studies.** *Ann Intern Med*. 2021;174:1592–1599 CrossRef Medline
14. Suzuki S. **Conditional relative odds ratio and comparison of accuracy of diagnostic tests based on 2 × 2 tables.** *J Epidemiol*. 2006;16:145–153 CrossRef Medline
15. IntHout J, Ioannidis JP, Borm GF. **The Hartung-Knapp-Sidik-Jonkman method for random effects meta-analysis is straightforward and considerably outperforms the standard DerSimonian-Laird method.** *BMC Med Res Methodol*. 2014;14:25 CrossRef Medline
16. Egger M, Davey Smith G, Schneider M, et al. **Bias in meta-analysis detected by a simple, graphical test.** *BMJ*. 1997;315:629–634 CrossRef Medline
17. Viechtbauer W, Cheung MW. **Outlier and influence diagnostics for meta-analysis.** *Res Synth Methods*. 2010;1:112–125 CrossRef Medline
18. Komada T, Naganawa S, Ogawa H, et al. **Contrast-enhanced MR imaging of metastatic brain tumor at 3 tesla: utility of T(1)-weighted SPACE compared with 2D spin echo and 3D gradient echo sequence.** *Magnetic resonance in medical sciences: MRMS: an official journal of Japan Society of Magnetic Resonance in Medicine*. 2008;7:13EP–21 CrossRef Medline
19. Kato Y, Higano S, Tamura H, et al. **Usefulness of contrast-enhanced T1-weighted sampling perfection with application-optimized contrasts by using different flip angle evolutions in detection of small brain metastasis at 3T MR imaging: Comparison with magnetization-prepared rapid acquisition.** *American Journal of Neuroradiology*. 2009;30:923EP–929 CrossRef
20. Danieli L, Riccitelli GC, Distefano D, et al. **Brain Tumor-enhancement visualization and morphometric assessment: A comparison of MPRAGE, SPACE, and VIBE MRI techniques.** *American Journal of Neuroradiology*. 2019;40:1140EP–1148 CrossRef Medline
21. Bae YJ, Choi BS, Lee KM, et al. **Efficacy of maximum intensity projection of contrast-enhanced 3D turbo-spin echo imaging with improved motion-sensitized driven-equilibrium preparation in the detection of brain metastases.** *Korean Journal of Radiology*. 2017;18:699EP–709 CrossRef Medline
22. Chen Zhou ZH, Salvador Alvarez E, Hilario A, et al. **Improved detection of brain metastases using contrast-enhanced 3D black-blood TSE sequences compared to post-contrast 3D T1 GRE: a comparative study on 1.5-T MRI.** *European Radiology*. 2025:8 CrossRef Medline
23. Lee S, Park DW, Lee JY, et al. **Improved motion-sensitized driven-equilibrium preparation for 3D turbo spin echo T1 weighted imaging after gadolinium administration for the detection of brain metastases on 3T MRI.** *British Journal of Radiology*. 2016;89:20150176 CrossRef Medline
24. Kongpromsuk S, Pitakvej N, Jittapiromsak N, et al. **Detection of brain metastases using alternative magnetic resonance imaging sequences: A comparison between SPACE and VIBE sequences.** *Asian Biomedicine*. 2020;14:27EP–35 CrossRef
25. Gule-Monroe M, Chasen N, Long JP, et al. **Diagnostic Confidence of Contrast-Enhanced T1-Weighted MRI for the Detection of Brain Metastases: 3D FSE-vs. 3D GRE-Based Sequences.** *AJNR American journal of neuroradiology*. 2024 CrossRef Medline
26. Nagao E, Yoshiura T, Hiwatashi A, et al. **3D turbo spin-echo sequence with motion-sensitized driven-equilibrium preparation for detection of brain metastases on 3T MR imaging.** *American Journal of Neuroradiology*. 2011;32:664EP–670 CrossRef Medline
27. Mugler JP, 3rd, Brookeman JR. **Theoretical analysis of gadopentetate dimeglumine enhancement in T1-weighted imaging of the brain: comparison of two-dimensional spin-echo and three-dimensional gradient-echo sequences.** *J Magn Reson Imaging*. 1993;3:761–769 CrossRef Medline
28. Majigsuren M, Abe T, Kageji T, et al. **Comparison of Brain Tumor Contrast-enhancement on T1-CUBE and 3D-SPGR Images.** *Magnetic resonance in medical sciences: MRMS: an official journal of Japan Society of Magnetic Resonance in Medicine*. 2016;15:34EP–40 CrossRef Medline
29. Kotecha R, Kutuk T, Abrams KJ, et al. **Dedicated SRS imaging improves brain metastases detection and reduces the intracranial relapse risk.** *Radiotherapy and Oncology*. 2022;170:S819EP–S820 CrossRef
30. Chkili S, Lefebvre Y, Chao SL, et al. **Optimization of workflow for detection of brain metastases at 3T: is a black-blood MTC prepared 3D T1 used alone robust enough to replace the combination of conventional 3D T1 and the black-blood 3D T1 MTC?** *Neuroradiology*. 2023;65:1133EP–1141 CrossRef Medline

ACCEPTED MANUSCRIPT

SUPPLEMENTARY MATERIAL

Table of Contents

Supplemental Material: Detailed peer-reviewed search strategy for each database **2**

MEDLINE, n=1727 2

EMBASE, n=2093 4

Cochrane Central Register of Controlled Trials, n=55 6

ClinicalTrials.gov, n=39 8

Google Scholar, n=146 9

PROSPERO International Prospective Registry of Systematic Reviews, n=6 10

Supplemental Table 1: Patient characteristics in included studies **12**

Supplemental Table 2: MR Imaging characteristics in included studies **13**

Supplemental Table 3: Diagnostic performance for detecting brain metastases, CNR, and inter-rater agreement in included studies **14**

Supplemental Table 4: Diagnostic performance for detecting brain metastases for each MR sequence, stratified by lesion size **16**

Supplemental Table 5: False positive counts and reasons across included studies **17**

Supplemental Table 6: Calculation methods for CNR in included studies **18**

Supplemental Material: Calculation method for detection OR **1G**

Supplemental Figure 1: Influence analyses for detection OR estimates **20**

Supplemental Figure 2: Forest plot of OR estimates after removal of outlier studies **21**

Supplemental Figure 3: Forest plot of OR estimates stratified by lesion size **22**

Supplemental Figure 4: Sensitivity analyses for sensitivity estimates **23**

Supplemental Figure 5: Funnel plots for sensitivity estimates **24**

Supplemental Figure 6: Forest plot of sensitivity estimates in 3D T1 TSE sequences, stratified by sequence technique **25**

Supplemental Figure 7: Risk of bias using QUADAS-2/QUADAS-C tools **26**

Supplemental Material: References of included studies **27**

ACCEPTED MANUSCRIPT

Supplemental Material: Detailed peer-reviewed search strategy for each database

MEDLINE, n=1727

Interface: Ovid

Search Screen: Advanced Search

Search modes: Boolean/Phrase

Database: Ovid MEDLINE(R) ALL <1946 to April 10, 2025>

#	Query	Results April 11, 2025
1	exp Central Nervous System Neoplasms/ [includes Brain Neoplasms]	220,403
2	exp Brain Diseases/sc [Secondary floating subheading]	16,780
3	exp Neoplasm Metastasis/ and (brain* or cerebr* or cerebell* or central nervous).mp.	9,231
4	((brain* or cerebr* or cerebell* or central nervous) adj5 cancer*).mp.	19,756
5	((brain* or cerebr* or cerebell* or central nervous) adj5 carcinoma*).mp.	3,676
6	((brain* or cerebr* or cerebell* or central nervous) adj5 malignan*).mp.	16,883
7	((brain* or cerebr* or cerebell* or central nervous) adj5 metast*).mp.	29,316
8	((brain* or cerebr* or cerebell* or central nervous) adj5 (micrometast* or micro-metast*)).mp.	68
9	((brain* or cerebr* or cerebell* or central nervous) adj5 neoplas*).mp.	160,846
10	((brain* or cerebr* or cerebell* or central nervous) adj5 (oligometast* or oligo-metast*)).mp.	162
11	((brain* or cerebr* or cerebell* or central nervous) adj5 tumo?r*).mp.	91,831
12	brain mets.mp.	42
13	(cranial adj5 metasta*).mp.	724
14	(dura mater adj5 metasta*).mp.	51
15	(intracranial adj5 metasta*).mp.	2,625
16	(leptomeninge* adj5 carcino*).mp.	887
17	leptomeninge* disease*.mp.	764
18	leptomeninge* metasta*.mp.	1,498
19	leptomeningeal glioneuronal tumo?r*.mp.	111
20	or/1-19 [Brain metastasis concept]	278,724
21	gradient* echo*.mp.	10,707
22	gradientecho.mp.	11
23	(gradient* adj3 (magnetic resonan* or MRI?)).mp.	2,035
24	MP-RAGE.mp.	269
25	MPRAGE.mp.	760

ACCEPTED MANUSCRIPT

26	**(proton spin* adj3 imag*).mp.**	**18**
27	**(proton spin* adj3 tomograp*).mp.**	**45**
28	**(sampling perfection and contrast? and angle evolution?).mp. [SPACE]**	**253**
29	**(SPACE adj10 (MRI* or magnetic resonance)).mp.**	**4,924**
30	**(spin adj3 (magnetic resonan* or MRI?)).mp.**	**3,370**
31	**spin echo*.mp.**	**16,992**
32	**spinecho*.mp.**	**85**
33	**or/21-32 [spin echo or gradient echo concept]**	**33,210**
34	**and/20,33**	**1,727**
35	**34 and ("35662657" or "31221635" or "26334511" or "25770904" or "23192164" or "22104961" or "21292797" or "19213825" or "18460844").ui. [search by PMID for target articles identified by researchers]**	**9**
36	**limit 34 to dt=20240408-20250411 [April 5, 2024 to April 11, 2025]**	**79**
37	**limit 34 to up=20240408-20250411 [April 5, 2024 to April 11, 2025]**	**1,727**

(9 target studies were picked up in search)

ACCEPTED MANUSCRIPT

EMBASE, n=2093

Interface: Ovid

Search Screen: Advanced Search

Search modes: Boolean/Phrase

Database: Embase Classic+Embase <1947 to 2025 Week 14>

#	Query	Results April 11, 2025
1	exp *central nervous system tumor/ [includes brain tumor, central nervous system cancer, meningeal tumor, others]	322,687
2	exp *metastasis/ and (brain* or cerebr* or cerebell* or central nervous).ti,ab,kf.	35,352
3	((brain* or cerebr* or cerebell* or central nervous) adj5 cancer*).ti,ab,kf.	30,155
4	((brain* or cerebr* or cerebell* or central nervous) adj5 carcinoma*).ti,ab,kf.	4,238
5	((brain* or cerebr* or cerebell* or central nervous) adj5 malignan*).ti,ab,kf.	25,310
6	((brain* or cerebr* or cerebell* or central nervous) adj5 metast*).ti,ab,kf.	50,852
7	((brain* or cerebr* or cerebell* or central nervous) adj5 (micrometast* or micro-metast*)).ti,ab,kf.	112
8	((brain* or cerebr* or cerebell* or central nervous) adj5 neoplas*).ti,ab,kf.	11,897
9	((brain* or cerebr* or cerebell* or central nervous) adj5 (oligometast* or oligo-metast*)).ti,ab,kf.	307
10	((brain* or cerebr* or cerebell* or central nervous) adj5 tumo?r*).ti,ab,kf.	134,478
11	brain mets.ti,ab,kf.	395
12	(cranial adj5 metasta*).ti,ab,kf.	1,329
13	(dura mater adj5 metasta*).ti,ab,kf.	77
14	(intracranial adj5 metasta*).ti,ab,kf.	4,008
15	(leptomeninge* adj5 carcino*).ti,ab,kf.	1,330
16	leptomeninge* disease*.ti,ab,kf.	1,623
17	leptomeninge* metasta*.ti,ab,kf.	2,388
18	leptomeningeal glioneuronal tumo?r*.ti,ab,kf.	195
19	or/1-18 [Brain metastasis concept]	409,609
20	gradient* echo*.ti,ab,kf.	14,471
21	gradientecho.ti,ab,kf.	125
22	(gradient* adj3 (magnetic resonan* or MRI?)).ti,ab,kf.	2,548
23	MP-RAGE.ti,ab,kf.	544
24	MPRAGE.ti,ab,kf.	2,121

ACCEPTED MANUSCRIPT

25	**(proton spin* adj3 imag*).ti,ab,kf.**	**18**
26	**(proton spin* adj3 tomograp*).ti,ab,kf.**	**14**
27	**(sampling perfection and contrast? and angle evolution?).ti,ab,kf. [SPACE]**	**289**
28	**(SPACE adj10 (MRI* or magnetic resonance)).ti,ab,kf.**	**6,600**
29	**(spin adj3 (magnetic resonan* or MRI?)).ti,ab,kf.**	**4,320**
30	**spin echo*.ti,ab,kf.**	**19,938**
31	**spinecho*.ti,ab,kf.**	**239**
32	**or/20-31 [spin echo or gradient echo concept]**	**43,287**
33	**and/19,32**	**2,093**

ACCEPTED MANUSCRIPT

Cochrane Central Register of Controlled Trials, n=55

Interface: Ovid

Search Screen: Advanced Search

Search modes: Boolean/Phrase

Database: EBM Reviews - Cochrane Central Register of Controlled Trials <March 2025>

#	Query	Results April 11, 2025
1	exp Central Nervous System Neoplasms/ [includes Brain Neoplasms]	3,555
2	exp Brain Diseases/sc [Secondary floating subheading]	1
3	exp Neoplasm Metastasis/ and (brain* or cerebr* or cerebell* or central nervous).mp.	393
4	((brain* or cerebr* or cerebell* or central nervous) adj5 cancer*).mp.	4,392
5	((brain* or cerebr* or cerebell* or central nervous) adj5 carcinoma*).mp.	433
6	((brain* or cerebr* or cerebell* or central nervous) adj5 malignan*).mp.	710
7	((brain* or cerebr* or cerebell* or central nervous) adj5 metast*).mp.	3,436
8	((brain* or cerebr* or cerebell* or central nervous) adj5 (micrometast* or micro-metast*)).mp.	2
9	((brain* or cerebr* or cerebell* or central nervous) adj5 neoplas*).mp.	3,382
10	((brain* or cerebr* or cerebell* or central nervous) adj5 (oligometast* or oligo-metast*)).mp.	28
11	((brain* or cerebr* or cerebell* or central nervous) adj5 tumo?r*).mp.	3,304
12	brain mets.mp.	60
13	(cranial adj5 metasta*).mp.	46
14	(dura mater adj5 metasta*).mp.	0
15	(intracranial adj5 metasta*).mp.	133
16	(leptomeninge* adj5 carcino*).mp.	29
17	leptomeninge* disease*.mp.	67
18	leptomeninge* metasta*.mp.	71
19	leptomeningeal glioneuronal tumo?r*.mp.	0
20	or/1-19 [Brain metastasis concept]	10,718
21	gradient* echo*.mp.	321
22	gradientecho.mp.	1
23	(gradient* adj3 (magnetic resonan* or MRI?)).mp.	48
24	MP-RAGE.mp.	26
25	MPRAGE.mp.	76
26	(proton spin* adj3 imag*).mp.	0
27	(proton spin* adj3 tomograp*).mp.	2
28	(sampling perfection and contrast? and angle evolution?).mp. [SPACE]	11

ACCEPTED MANUSCRIPT

29	**(SPACE adj10 (MRI* or magnetic resonance)).mp.**	**213**
30	**(spin adj3 (magnetic resonan* or MRI?)).mp.**	**219**
31	**spin echo*.mp.**	**366**
32	**spinecho*.mp.**	**4**
33	**or/21-32 [spin echo or gradient echo concept]**	**1,094**
34	**and/20,33**	**55**

ACCEPTED MANUSCRIPT

ClinicalTrials.gov, n=39

Cinicaltrials.gov

Provider: US National Library of Medicine

Interface: website search at https://www.clinicaltrials.gov/

Search modes: Boolean/Phrase

Details	Date	# of Results	Search Query
	04/11/2025	39	spin or gradient | brain or cerebral

ACCEPTED MANUSCRIPT

Google Scholar,

n=146 Google LLC

https://scholar.google.ca/

Query	Results April 11, 2025
All searches with filter "Since 2024"	Results April 11, 2025
brain metastases spin echo	About 2,180 results
brain metastases gradient echo	About 3,290 results
spin echo gradient echo brain	About 12,800 results
spin echo gradient echo cerebral	About 12,400 results
brain spin echo gradient echo	About 10,300 results
cerebral spin echo gradient echo	About 11,900 results
spin echo metastasis	About 3,790 results
gradient echo metastasis	About 5,400 results
brain metastasis SPACE	About 17,300 results
brain metastasis SPACE MRI	About 13,000 results

(42 results selected by information specialist)

Query	Results April 8, 2024
brain metastases spin echo	About 27,500 results
brain metastases gradient echo	About 28,600 results
spin echo gradient echo brain	About 234,000 results
spin echo gradient echo cerebral	About 163,000 results
brain spin echo gradient echo	About 217,000 results
cerebral spin echo gradient echo	About 156,000 results
spin echo metastasis	About 54,600 results
gradient echo metastasis	About 48,900 results
brain metastasis SPACE	About 445,000
brain metastasis SPACE MRI	About 88,100 results
brain metastasis MPRAGE	About 3,260 results

(104 results selected for screening by Information Specialist)

ACCEPTED MANUSCRIPT

PROSPERO International Prospective Registry of Systematic Reviews, n=6

Provider – UK University of York Centre for Reviews and Dissemination

Search Screen – Advanced Search

Search modes – Boolean/Phrase

Web address - https://www.crd.york.ac.uk/prospero/#searchadvanced

Line #	Search for	Hits April 11, 2025
1	MeSH DESCRIPTOR Central Nervous System Neoplasms EXPLODE	1053
2	MeSH DESCRIPTOR Brain Neoplasms EXPLODE ALL TREES	839
3	MeSH DESCRIPTOR Neoplasm Metastasis EXPLODE ALL TREES	525
4	((brain*) NEAR5 (cancer* or carcinoma* or malignan* or metast* or micrometast* or micro-metast* or neoplasm* or oligometast* or oligometast* or tumor* or tumour*))	2005
5	((cerebr*) NEAR5 (cancer* or carcinoma* or malignan* or metast* or micrometast* or micro-metast* or neoplasm* or oligometast* or oligo-metast* or tumor* or tumour*))	223
6	((cerebell*) NEAR5 (cancer* or carcinoma* or malignan* or metast* or micrometast* or micro-metast* or neoplasm* or oligometast* or oligo- metast* or tumor* or tumour*))	46
7	((CNS) NEAR5 (cancer* or carcinoma* or malignan* or metast* or micrometast* or micro-metast* or neoplasm* or oligometast* or oligo-metast* or tumor* or tumour*))	268
8	brain mets	5
9	(cranial NEAR5 metasta*)	10
10	(dura mater NEAR5 metasta*)	0
11	(intracranial NEAR5 metasta*)	42
12	(leptomeninge* NEAR5 carcino*)	6
13	(leptomeninge* disease*)	20
14	(leptomeninge* metasta*)	19
15	(leptomeningeal) NEAR3 (tumor OR tumour)	1
16	(glioneuronal) NEAR3 (tumor OR tumour)	3
17	#16 or #1 or #2 or #3 or #4 or #5 or #6 or #7 or #8 or #9 or #10 or #11 or #12 or #13 or #14 or #15	3105
18	gradient* echo*	13
19	gradientecho	0
20	gradient* NEAR5 (magnetic resonan* OR MRI)	1
21	MP-RAGE OR MPRAGE	6
22	(spin*) NEAR3 imag*	87
23	(spin*) NEAR3 tomograp*	22

ACCEPTED MANUSCRIPT

24	**sampling perfection contrast angle evolution***	**0**
25	**SPACE NEAR10 (MRI* OR magnetic)**	**31**
26	**spin echo***	**20**
27	**spin NEAR3 (magnetic OR MRI)**	**23**
28	**spinecho**	**1**
29	**#18 or #19 or #20 or #21 or #22 or #23 or #24 or #25 or #26 or #27 or #28**	**182**
30	**#29 and #17**	**6**

ACCEPTED MANUSCRIPT

Supplemental Table 1: Patient characteristics in included studies

First Author and Year	No. of patients	No. of brain metastases	Age[a]	Female[b]	Sites of primary neoplasm	Level of Analysis
Komada 2008	22	11	64.9 (39–87)	7 (32%)	Lung (n=19, 86%), Breast (n=2, 9%), Germ cell (n=1, 5%)	Brain Segment
Kato 2009	16	170	57.3 (42–82)	9 (56%)	Lung (n=11, 69%), Breast (n=1, 6%), Colon (n=1, 6%), Pancreas (n=1, 6%), Kidney (n=1, 6%), Testis (n=1, 6%)	Lesion
Nagao 2011	17	450*	62 (35–81)	13 (38%)	Lung (n=9, 53%), Breast (n=3, 18%), Colon (n=2, 12%), Kidney (n=2, 12%), Stomach (n=1, 6%)	Lesion
Park 2012	35	242	58.1 (30–75)	18 (51%)	Lung (n=23, 66%), Breast (n=12, 34%)	Lesion
Reichert 2013	17	219	64 ± 14	NR	NR	Lesion
Kwak 2015	12	72	62.4 (50–77)	3 (25%)	Lung (n=11, 92%), Breast (n=1, 8%)	Lesion
Lee 2016	14	96	64.5 (37–87)	5 (36%)	Lung (n=10, 71%), Melanoma (n=2, 14%), Lymphoma (n=1, 7%), Stomach (n=1, 7%), Bladder (n=1, 7%)	Lesion
Bae 2017	30	365	60.6 (28–77)	18 (60%)	Lung (n=26, 87%), Breast (n=2, 7%), Ovary (n=1, 3%), Rectum (n=1, 3%)	Lesion
Danieli 2019	8	16	NR	NR	Lung (n=7), Breast (n=3), Melanoma (n=1), Colorectal (n=2), Kidney (n=3)	Lesion
Kim 2019	71	569	64.3 (40–84)	25 (35%)	Lung (n=53), Breast (n=8), Colon (n=2), Prostate (n=2), Kidney (n=1), Gastric (n=1), Ovary (n=1), Endometrium (n=1), Cervix (n=1), External auditory canal (n=1)	Lesion
Kongpromsuk 2020	27	424	55.0 ± 14.3	16 (59%)	Lung (n=18, 67%), Breast (n=4, 15%), Head & neck (n=2, 7%), Cervical (n=1, 4%), Ovarian (n=1, 4%), HCC (n=1, 4%)	Lesion
Jun 2022	53	190	59.6 (25–77)	16 (30%)	Lung (n=43, 81%), Breast (n=6, 11%), Esophageal (n=2, 4%), Rectal (n=1, 2%), Cervical (n=1, 2%)	Lesion
Fu 2022	43	94	55.3 (32–73)	18 (42%)	Lung (n=37, 86%), Breast (n=6, 14%)	Lesion
Gule-Monroe 2024	72	832	61 (21–86)	40 (55%)	Lung (n=29, 40%), Breast (n=16, 22%), Melanoma (n=13, 18%), Colon (n=1, 1%), Renal (n=7, 10%) Other (n=6, 8%)	Lesion
Chen Zhou 2025	107	588	60.8 ± 13.2	52 (49%)	Lung (n=55, 51.4%), Breast (n=18, 16.8%), Melanoma (n=10, 9.3%), Other (n=24, 22.5%)	Lesion

Note: - NR indicates 'not reported in study'. * Aggregate total from 9 compound readings of 50 metastases.

[a] Data are mean ± SD or mean (min-max).

[b] Data are frequencies (percentage).

ACCEPTED MANUSCRIPT

Supplemental Table 2: MR Imaging characteristics in included studies

First Author and Year	MR Field Strength	MR Vendor and machine (coil)	3D T1 TSE sequence name	3D T1 GRE sequence name	Voxel (mm^3)	IV Contrast type and dose	Sequence order
Komada 2008	3T	Siemens Magnetom Trio (phased-array head coil)	SPACE	MPRAGE	1	Gd-DTPA 0.2 mL/kg	Alternated or randomized
Kato 2009	3T	GE Signa Excite HD (8-channel head coil)	SPACE	MPRAGE	1	Gd-DTPA 0.1 mmol/kg	Alternated or randomized
Nagao 2011	3T	Philips Achieva (8-channel SENSE head coil)	TSE-MSDE	MPRAGE	1	Gd-DTPA 0.1 mmol/kg	Alternated or randomized
Park 2012	3T	Siemens Magnetom Trio (12-channel phased-array head coil)	BB-ssTSE with VFA	MPRAGE	1	Gd-DTPA 0.2 mmol/kg	Fixed order (BB-ssTSE first)
Reichert 2013	3T	Siemens Magnetom Trio (32-channel phased-array head coil)	SPACE	MPRAGE	1.1	Gd-DTPA 0.1 mmol/kg	Alternated or randomized
Kwak 2015	3T	Siemens Verio (12-channel head coil)	SPACE	MPRAGE	1.2	Gadobutrol 0.1 mL/kg	Alternated or randomized
Lee 2016	3T	Philips (model and coil NR)	TSE-iMSDE	C-GRE	2	Gd-DTPA 0.1 mmol/kg	Fixed order (C-GRE first)
Bae 2017	3T	Philips Ingenia (32-channel SENSE head coil)	TSE-iMSDE	3D-GRE	1	Gadobutrol 0.1 mmol/kg	Alternated or randomized
Danieli 2019	3T	Siemens Magnetom Skyra (20-channel head coil)	SPACE	MPRAGE	1	Gadobutrol 0.1 mL/kg	Alternated or randomized
Kim 2019	3T	Siemens Magnetom Skyra (20-channel head coil)	DANTE-SPACE	MPRAGE	0.72	Gadoterate meglumine 0.1 mmol/kg	Alternated or randomized
Kongpromsuk 2020	3T	Siemens Magnetom Skyra (20-channel head-neck coil)	SPACE	VIBE	0.98	Gadoterate meglumine 0.1 mmol/kg	Fixed order (SPACE first)
Jun 2022	3T	Philips Elition (16-channel neurovascular coil)	3D BB TSE-MSDE	3D TFE	1	Gadopentetate dimeglumine 0.1 mmol/kg	Alternated or randomized
Fu 2022	3T	Siemens Magnetom Skyra (20-channel head-neck coil)	DANTE-SPACE	MPRAGE	0.94	Gadobutrol 0.1 mL/kg	Alternated or randomized
Gule-Monroe 2024	3T	Siemens Magnetom Skyra (20-channel head coil)	SPACE	3D FLASH	1	Gadobutrol 0.1 mmol/kg	Alternated or randomized
Chen Zhou 2025	1.5T	GE Signa Artist (19-ch head coil)	3D BB TSE-MSDE	3D-FSPGR	1	Gadobutrol 0.1 mmol/kg	Alternated or randomized

ACCEPTED MANUSCRIPT

Note: - NR indicates 'not reported in study'; SPACE, Sampling Perfection with Application-Optimized Contrasts by using different flip angle Evolutions; BB-ssTSE with VFA, Black Blood- single-slab TSE with Variable Flip Angle; MALTVE, Magnetization Transfer Prepared Spin Echo-Like Contrast Volume Examination; TSE-(i)MSDE, TSE with (improved) Motion-Sensitized Driven-Equilibrium; DANTE, Delay Alternating with Nutation for Tailored Excitation; FSPGR, Fast Spoiled Gradient-Echo; C-GRE, Conventional Gradient Recalled Echo; BB, Black Blood.

Supplemental Table 3: Diagnostic performance for detecting brain metastases, CNR, and inter-rater agreement in included studies

First Author and Year	No. of Mets	3D T1 TSE								3D T1 GRE								No. of raters
		TP	FN	FP	TN	Se	Sp	CNR[a]	Reported Agreement[b]	TP	FN	FP	TN	Se	Sp	CNR[a]	Reported Agreement[b]	
Komada 2008	11	10	1	0	68	90.9%	98.6%	39.9 ± 35.9	0.74	9	2	1	69	81.8%	100%	12.2 ± 11.8	0.65	2
Kato 2009	170	168	2	12	168	98.8%	93.3%	3.0 ± 1.9	NR	118	52	17	163	69.4%	90.6%	2.6 ± 2.2	NR	2
Nagao 2011	450[c]	370	80	NR	NR	82.2%	NR	≈ 10 ± 4[d]	NR	294	156	NR	NR	65.3%	NR	≈ 8 ± 3[d]	NR	9
Park 2012	242	236	6	0	NR	97.5%	NR	18.8 ± 6.3	0.99	200	42	0	NR	82.6%	NR	16.6 ± 5.6	0.91	2
Reichert 2013[e]	219	213	6	4	NR	97.2%	NR	NR	0.88	159	60	0	NR	73.6%	NR	NR	0.86	2
Kwak 2015[e]	72	65	7	3	NR	90.3%	NR	NR	0.72	56	16	2	NR	77.8%	NR	NR	0.65	2
Lee 2016	96	96	0	1	NR	100%	NR	NR	NR[f]	85	11	1	NR	88.5%	NR	NR	NR[f]	2
Bae 2017[e]	365	354	11	6	89	97.0%	93.7%[g]	NR	0.86	235	130	1	NR	64.4%	98.9%	NR	0.72	2
Danieli 2019	16	16	0	0	NR	100%	NR	17.2 (13.6-21.3)	NR	13	3	0	NR	81.3%	NR	9.30 (6.77-12.3)	NR	2
Kim 2019[e]	569	514	55	18	NR	90.3%	NR	52.3 ± 43.1	0.99	343	226	10	NR	60.3%	NR	17.5 ± 19.3	0.98	2
Kongpromsuk 2020	424	423	1	3	NR	99.8%	NR	NR	1.00	371	7	3	NR	98.1%	NR	NR	1.00	2
Jun 2022	190	190	0	0	NR	100%	NR	NR	0.82	169	21	0	NR	88.9%	NR	NR	0.66	2
Fu 2022	94	82	12	2	NR	87.2%	NR	89.1 ±194.8	0.97	52	42[h]	0	NR	55.3%[h]	NR	19.6 ± 24.8	0.96	2
Gule-Monroe 2024	832	832	0	NR	NR	100%	NR	22.9 (15.1-33.5)	0.96	723	109	NR	NR	86.9%	NR	15.5 (11.2-22.0)	0.87	5
Chen Zhou 2025	588	588	0	NR	NR	100%	NR	1.67 ± 0.85	0.90 (0.86-0.94)	408	180	NR	NR	69.4%	NR	1.38 ± 1.07	0.95 (0.93-0.98)	2

ACCEPTED MANUSCRIPT

Supplemental Table 3: Diagnostic performance for detecting brain metastases, CNR, and inter-rater agreement in included studies (cont'd)

Note: - NR indicates 'not reported in study'; TP, true positives; FN, false negatives; FP, false positives; TN, true negatives; Se, sensitivity; Sp, specificity; CNR, Contrast-to-noise-ratio (lesion-white matter); Mets, brain metastases.

[a] Data are mean CNR ± SD or median CNR (IQR).
[b] Reliability agreement estimates (usually κ statistics or ICC depending on the study), with 95% IC whenever reported.
[c] Total number of lesions (50) x 9 readers (Aggregated total).
[d] Approximate CNR estimate extrapolated from a bar plot.
[e] For these studies, no consensus readings were available (in addition to the individual observer readings). Results from the observer with the highest sensitivity were extracted in this table.
[f] Authors mentioned 'very high percent agreements' and deemed unnecessary to report reliability coefficients.
[g] Re-estimated specificity from available raw data, as the reported estimate was incongruent with raw data.
[h] Re-estimated FN and specificity from available raw data.

ACCEPTED MANUSCRIPT

Supplemental Table 4: Diagnostic performance for detecting brain metastases for each MR sequence, stratified by lesion size

First Author and Year	No. of metastases	Lesion size	3D T1 TSE						3D T1 GRE					
			TP	FN	FP	TN	Se	Sp	TP	FN	FP	TN	Se	Sp
Kato 2009	115	<5 mm	113	2	NR	NR	98.3%	NR	66	49	NR	NR	57.4%	NR
	55	≥5 mm	55	0	NR	NR	100%	NR	52	3	NR	NR	94.5%	NR
Nagao 2011	279	<5 mm	204	75	NR	NR	73.1%	NR	128	151	NR	NR	45.9%	NR
	171	≥5 mm	166	5	NR	NR	97.1%	NR	166	5	NR	NR	97.1%	NR
Park 2012	153	≤5 mm	148	5	0	NR	96.7%	NR	111	42	0	NR	72.5%	NR
	89	>5 mm	88	1	0	NR	98.9%	NR	89	0	0	NR	100%	NR
Bae 2017	237	≤3 mm	226	11	1	72	95.3%	98.7%	113	124	1	72	47.7%	98.6%
	128	>3 mm	128	0	5	17	100%	77.3%[a]	122	6	0	22	95.3%	100%[a]
Kim 2019	373	<5 mm	328	45	NR	NR	87.9%	NR	175	198	NR	NR	46.9%	NR
	196	≥5 mm	186	10	NR	NR	94.9%	NR	168	28	NR	NR	85.7%	NR
Jun 2022	105	<5 mm	105	0	0	NR	100%	NR	84	21	0	NR	80.0%	NR
	85	≥5 mm	85	0	0	NR	100%	NR	85	0	0	NR	100%	NR
Chen Zhou 2025	378	<5 mm	378	0	NR	NR	100%	NR	216	162	NR	NR	57.1%	NR
	211	≥5 mm	211	0	NR	NR	100%	NR	195	16	NR	NR	92.4%	NR

Note: - NR indicates 'not reported in study'; TP, true positives; FN, false negatives; FP, false positives; TN, true negatives; Se, sensitivity; Sp, specificity.

*** Re-estimated values from raw data. The reported estimates were incongruent with the raw data.**

ACCEPTED MANUSCRIPT

Supplemental Table 5: False positive counts and reasons across included studies

First Author and Year	3D T1 TSE		3D T1 GRE	
	False positive counts	Reported reasons	False positive counts	Reported reasons
Komada 2008	0	None	1	Cortical vessel
Kato 2009	12	Venous sinus, deep venous structures, choroid plexus, partial-volume/pulsation artifacts	17	Cortical vessels, venous sinus, choroid plexus, infarction, artifacts
Park 2012	0	N/A	0	N/A
Reichert 2013	4	NR	0	N/A
Kwak 2015	3	Vessels (incomplete suppression, residual flow artifact)	2	Vessels, artifacts
Lee 2016	1	Enhancing sagittal sinus	1	cortical vessel
Bae 2017	6	Vessels (veins), dural sinus, motion/flow artifacts	1	Vessels
Danieli 2019	0	N/A	0	N/A
Kim 2019	18	vessels (incomplete suppression), flow artifacts	10	vessels, flow artifacts
Kongpromsuk 2020	3	Vessels (mimicking leptomeningeal disease)	3	Vessels (mimicking leptomeningeal disease)
Jun 2022	0	N/A	0	N/A
Fu 2022	2	Vessels (incomplete suppression of cortical veins)	0	N/A
TOTAL	49		35	

Note: - NR indicates 'Not reported in study'; N/A, not applicable.

ACCEPTED MANUSCRIPT

Supplemental Table 6: Calculation methods for CNR in included studies

Studies (Author s Year)	CNR formula (lesion-background)
Komada 2008	$\frac{SI_{lesion} - SI_{white\ matter}}{SD_{air}}$
Kato 2009	$\frac{SI_{lesion} - SI_{white\ matter}}{SD_{lesion}}$
Nagao 2011, Park 2012	$\frac{SI_{lesion} - SI_{white\ matter}}{0.5 \times (SD_{lesion} + SD_{white\ matter})}$
Kim 2019, Danieli 2019, Fu 2022, Gule-Monroe 2024, Chen Zhou 2025	$\frac{SI_{lesion} - SI_{white\ matter}}{SD_{white\ matter}}$

Note-. SI_{lesion} and $SI_{white\ matter}$ represent the mean signal intensities of the enhancing lesion and surrounding white matter respectively; SD_{lesion}, the standard deviation of SI_{lesion}; $SD_{white\ matter}$, the standard deviation of $SI_{white\ matter}$; and SD_{air}, the standard deviation of signal intensity captured in the background, outside the head.

ACCEPTED MANUSCRIPT

Supplemental Material: Calculation method for detection OR

As only patients with intracranial metastases were included, diagnostic performance could only be evaluated using true positives (TP) and false negatives (FN), allowing estimation of sensitivity alone.

The odds of lesion detection among diseased cases only were expressed as:

$$Odds = \frac{Sensitivity}{1 - Sensitivity} = \frac{TP}{FN}$$

For each study, a conditional detection OR comparing TSE to GRE was calculated as follows:

$$OR = \frac{TP_{TSE}/FN_{SE}}{TP_{GRE}/FN_{GRE}} = \frac{TP_{TSE} \times FN_{GRE}}{TP_{GRE} \times FN_{TSE}}$$

This conditional detection OR should be interpreted as comparative sensitivity among diseased lesions, rather than as comprehensive diagnostic accuracy.

For meta-analytic purposes, the log(OR) was computed as the difference between log-transformed odds of detection:

$$\mathrm{Log(OR)} = \log\left(\frac{\mathrm{TP_{TSE}}}{\mathrm{FN_{TSE}}}\right) - \log\left(\frac{\mathrm{TP_{GRE}}}{\mathrm{FN_{GRE}}}\right)$$

A continuity correction of 0.5 was applied to any zero cell. The standard error (StEr) of the log(OR) was estimated using a Wald approximation:

$$\mathrm{StEr(Log(OR))} = \sqrt{\frac{1}{\mathrm{TP_{TSE}}} + \frac{1}{\mathrm{FN_{TSE}}} + \frac{1}{TP_{GRE}} + \frac{1}{FN_{GRE}}}$$

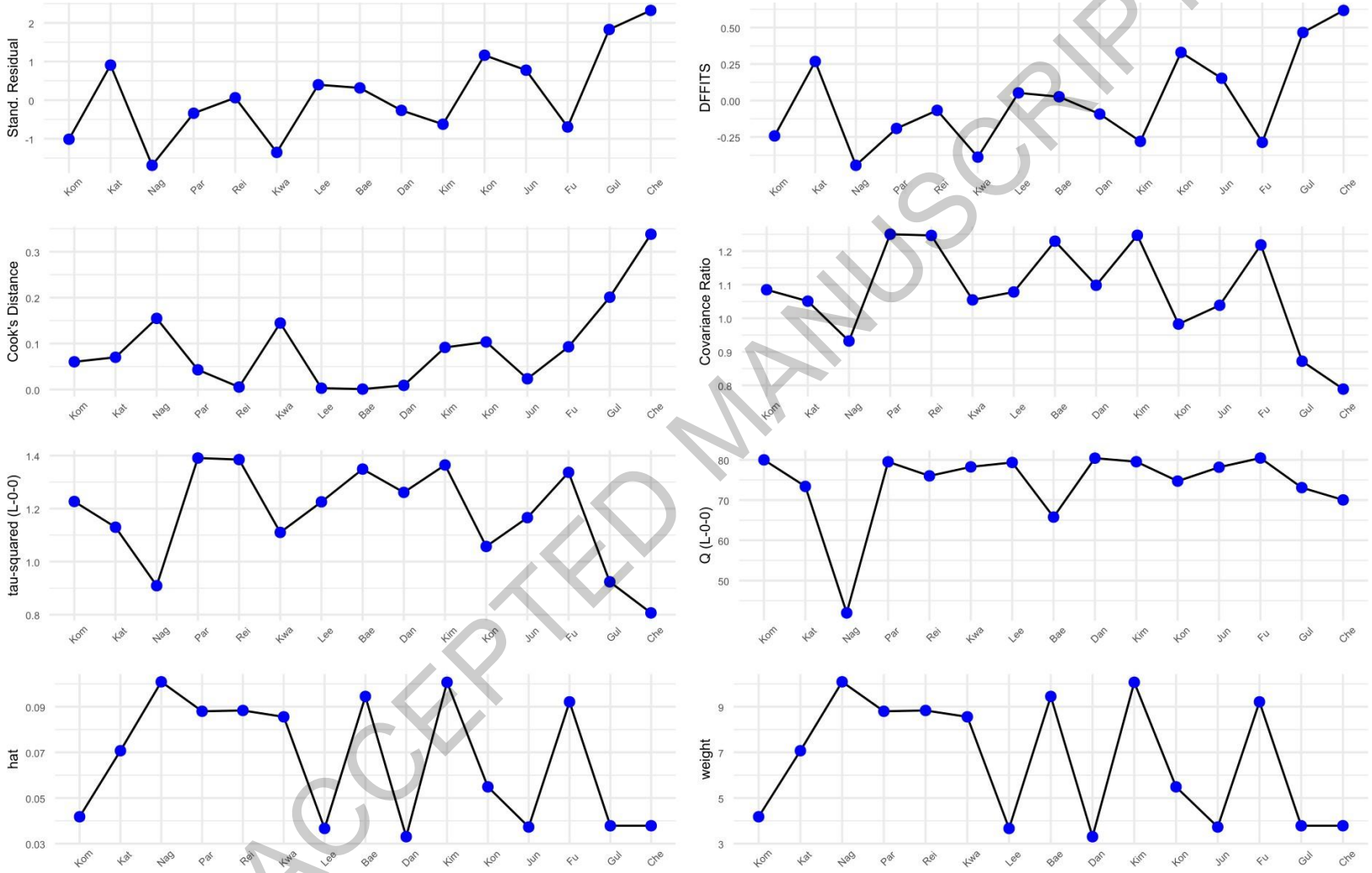
The 95% CI was calculated on the log scale as:

$$95\%\mathrm{CI(log(OR))} = \mathrm{log(OR)} \pm 1.96 * \mathrm{StEr(Log(OR))}$$

and was exponentiated to obtain the 95% CI on the OR scale. An OR greater than 1 indicates higher odds of lesion detection with TSE compared with GRE among diseased cases.

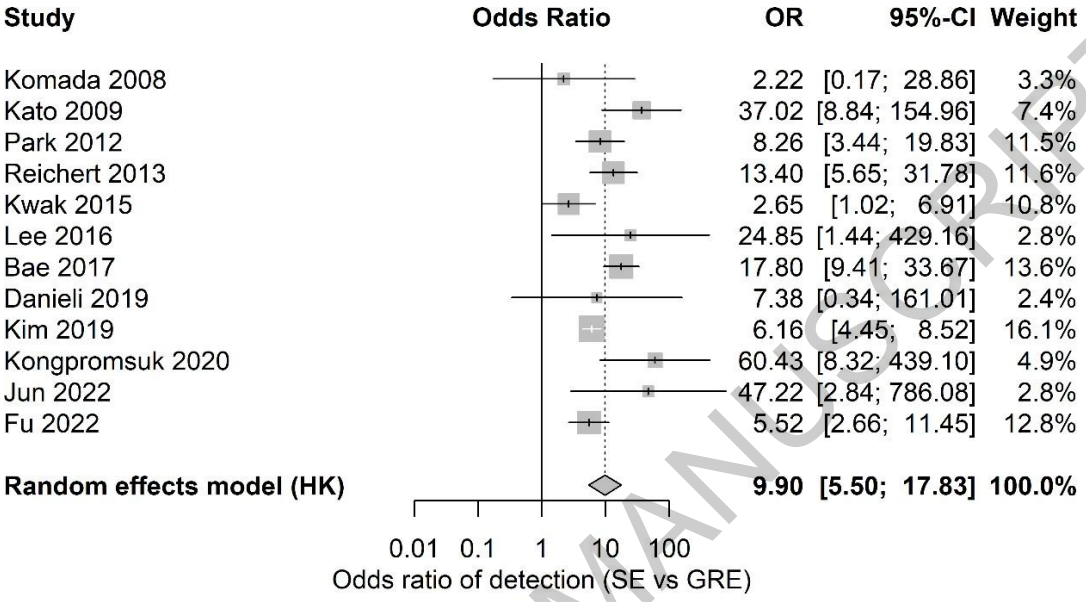
ACCEPTED MANUSCRIPT

Supplemental Figure 1: Influence analyses for detection OR estimates



ACCEPTED MANUSCRIPT

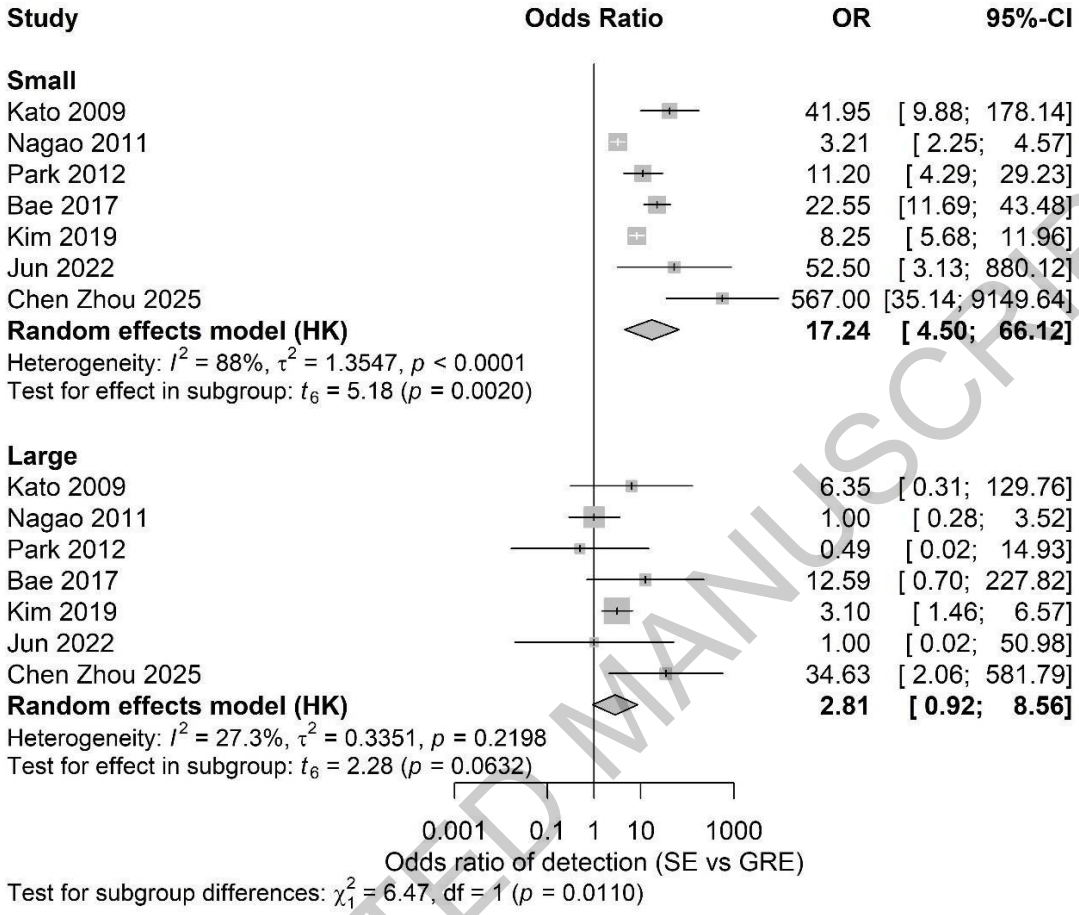
Supplemental Figure 2: Forest plot of OR estimates after removal of outlier studies



Heterogeneity: I^2 = 60.0%, τ^2 = 0.4078, p = 0.0039
Test for overall effect: t_{11} = 8.58 (p < 0.0001)

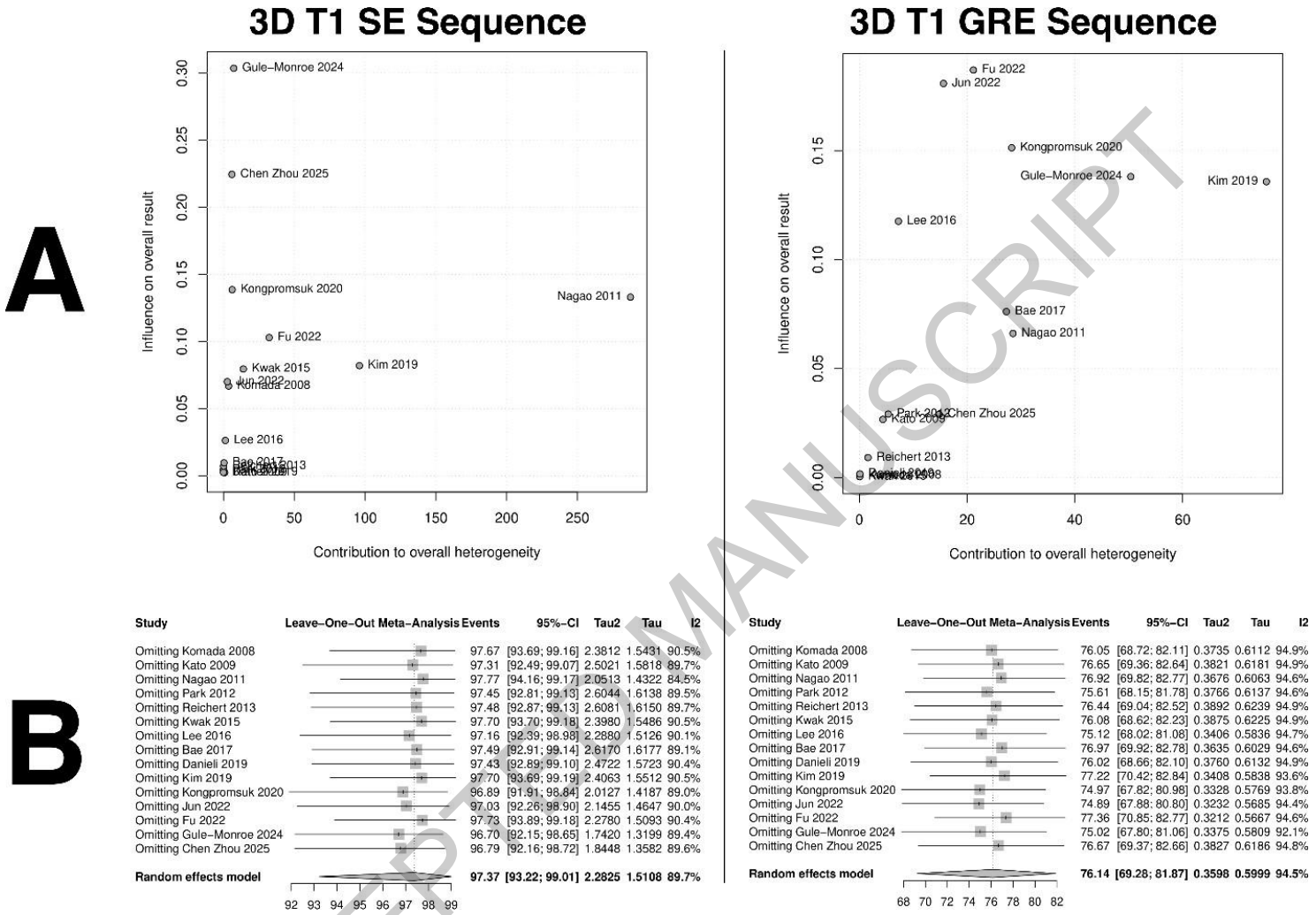
ACCEPTED MANUSCRIPT

Supplemental Figure 3: Forest plot of OR estimates stratified by lesion size



ACCEPTED MANUSCRIPT

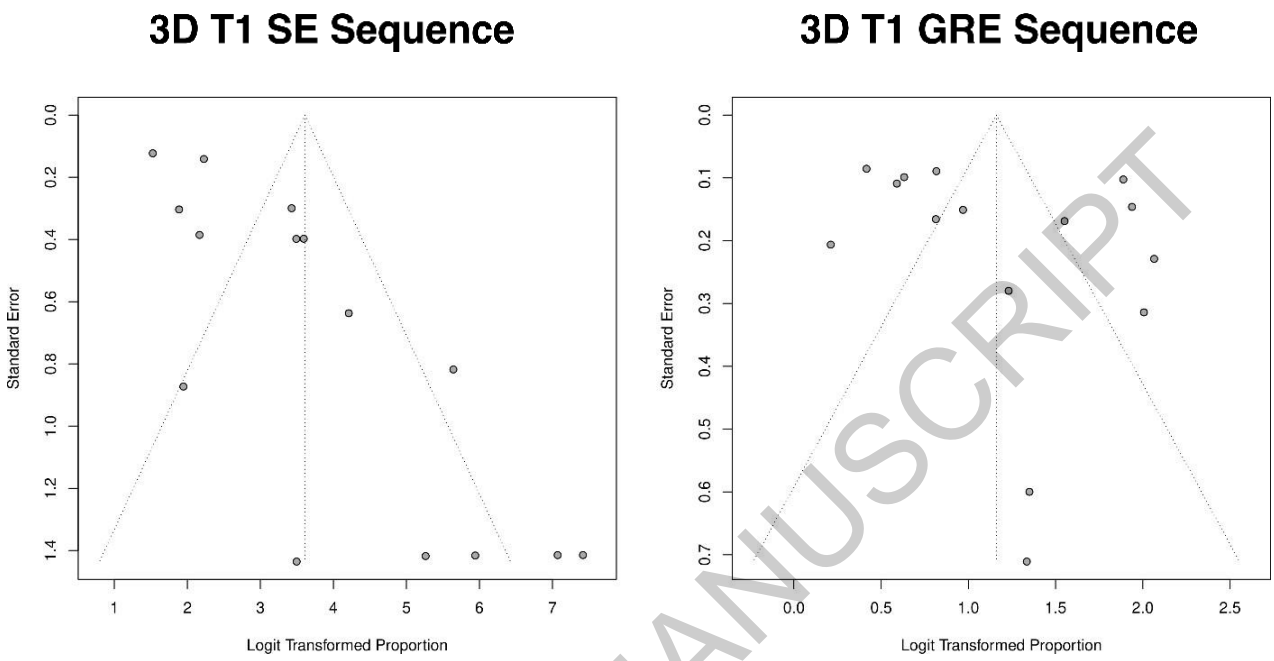
Supplemental Figure 4: Sensitivity analyses for sensitivity estimates



Baujat plots (A) and 'Leave-one-out' forest plots (B) of sensitivity estimates comparing TSE and GRE-based sequences for detection of intracranial metastases.

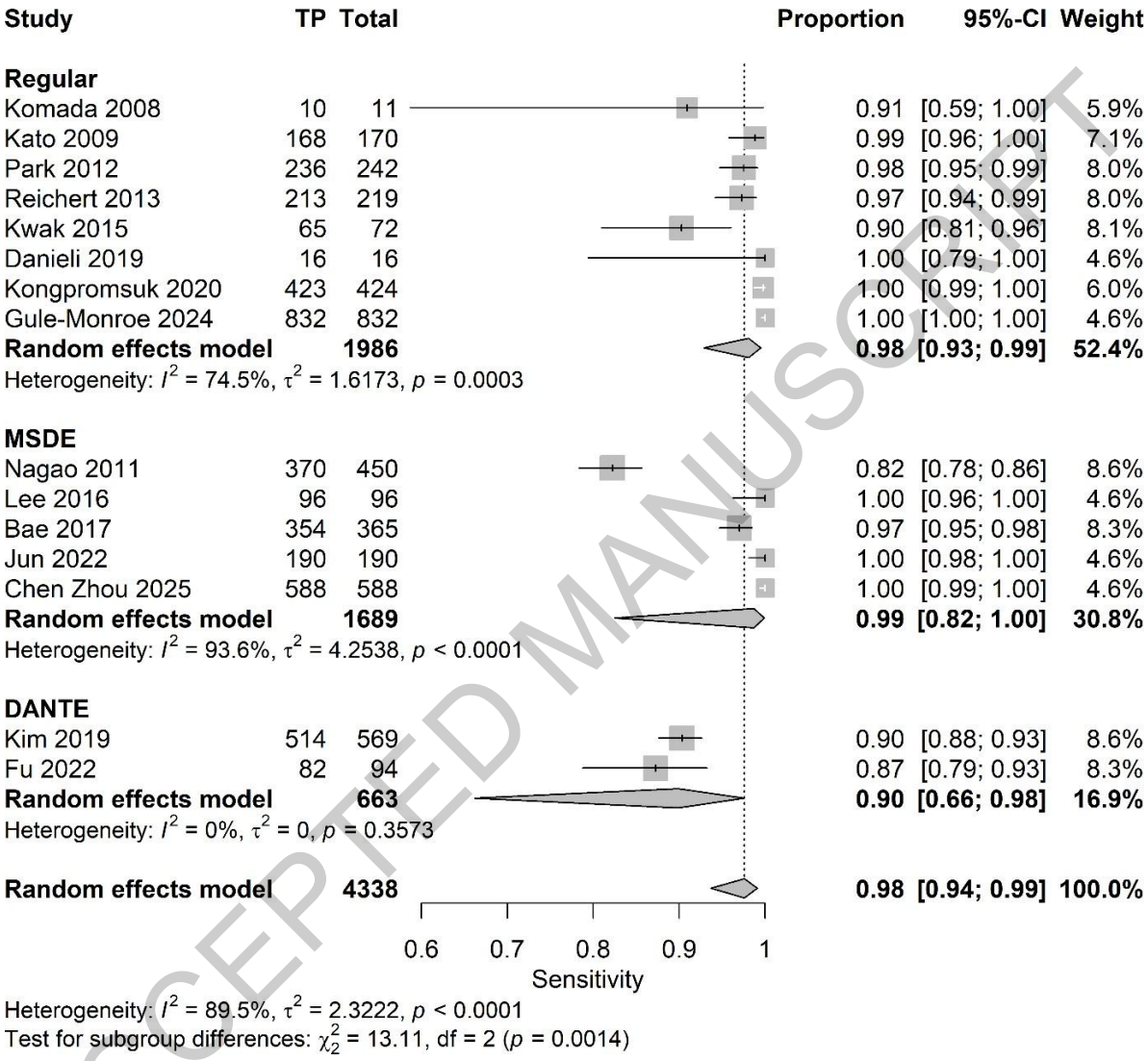
ACCEPTED MANUSCRIPT

Supplemental Figure 5: Funnel plots for sensitivity estimates



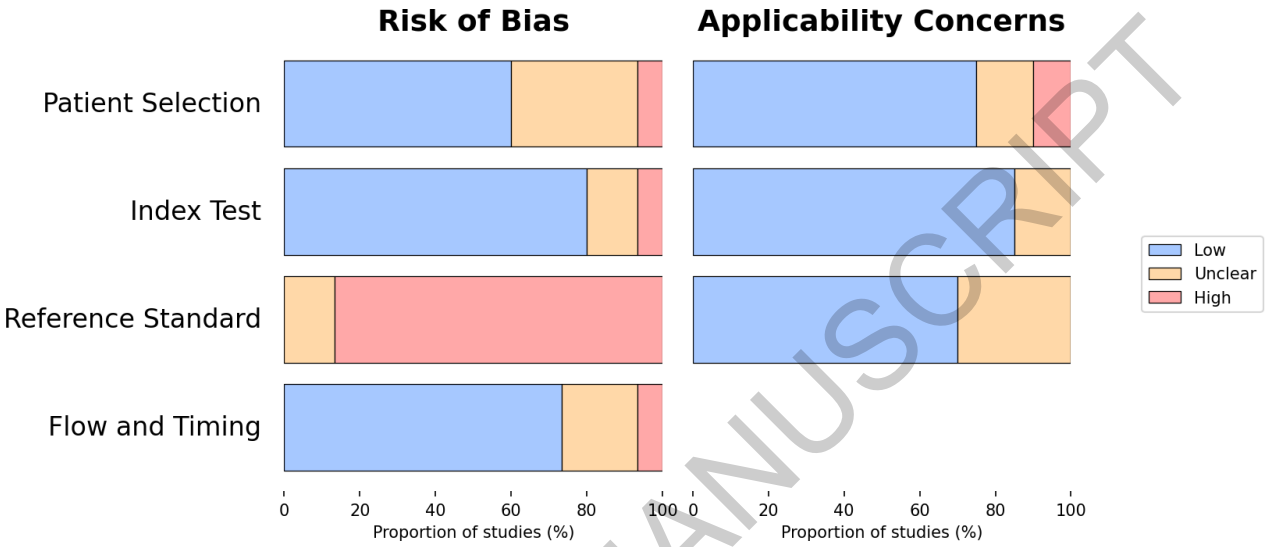
ACCEPTED MANUSCRIPT

Supplemental Figure 6: Forest plot of sensitivity estimates in 3D T1 TSE sequences, stratified by sequence technique



ACCEPTED MANUSCRIPT

Supplemental Figure 7: Risk of bias using QUADAS-2/QUADAS-C tools



ACCEPTED MANUSCRIPT

Supplemental Material: References of included studies

1. Komada T, Naganawa S, Ogawa H, et al. Contrast-enhanced MR imaging of metastatic brain tumor at 3 tesla: utility of T(1)-weighted SPACE compared with 2D spin echo and 3D gradient echo sequence. *Magnetic resonance in medical sciences : MRMS : an official journal of Japan Society of Magnetic Resonance in Medicine.* 2008;7:13EP-21. DOI: https://doi.org/https://dx.doi.org/10.2463/mrms.7.13

2. Kato Y, Higano S, Tamura H, et al. Usefulness of contrast-enhanced T1-weighted sampling perfection with application-optimized contrasts by using different flip angle evolutions in detection of small brain metastasis at 3T MR imaging: Comparison with magnetization-prepared rapid acquisition. *American Journal of Neuroradiology.* 2009;30:923EP-929. DOI: https://doi.org/https://dx.doi.org/10.3174/ajnr.A1506

3. Nagao E, Yoshiura T, Hiwatashi A, et al. 3D turbo spin-echo sequence with motion-sensitized driven-equilibrium preparation for detection of brain metastases on 3T MR imaging. *American Journal of Neuroradiology.* 2011;32:664EP-670. DOI: https://doi.org/https://dx.doi.org/10.3174/ajnr.A2343

4. Park J, Kim J, Yoo E, et al. Detection of small metastatic brain tumors: Comparison of 3D contrast- enhanced whole-brain black-blood imaging and MP-RAGE imaging. *Investigative Radiology.* 2012;47:136EP-141. DOI: https://doi.org/https://dx.doi.org/10.1097/RLI.0b013e3182319704

5. Reichert M, Morelli JN, Runge VM, et al. Contrast-enhanced 3-dimensional SPACE versus MP-RAGE for the detection of brain metastases: Considerations with a 32-channel head coil. *Investigative Radiology.* 2013;48:55EP-60. DOI: https://doi.org/https://dx.doi.org/10.1097/RLI.0b013e318277b1aa

6. Kwak HS, Hwang S, Chung GH, et al. Detection of small brain metastases at 3 T: Comparing the diagnostic performances of contrast-enhanced T1-weighted SPACE, MPRAGE, and 2D FLASH imaging. *Clinical Imaging.* 2015;39:571EP-575. DOI: https://doi.org/https://dx.doi.org/10.1016/j.clinimag.2015.02.010

7. Lee S, Park DW, Lee JY, et al. Improved motion-sensitized driven-equilibrium preparation for 3D turbo spin echo T1 weighted imaging after gadolinium administration for the detection of brain metastases on 3T MRI. *The British journal of radiology.* 2016;89:20150176. DOI: https://doi.org/https://dx.doi.org/10.1259/bjr.20150176

8. Bae YJ, Choi BS, Lee KM, et al. Efficacy of maximum intensity projection of contrast-enhanced 3D turbo-spin echo imaging with improved motion-sensitized driven-equilibrium preparation in the detection of brain metastases. *Korean Journal of Radiology.* 2017;18:699EP-709. DOI: https://doi.org/https://dx.doi.org/10.3348/kjr.2017.18.4.699

9. Danieli L, Riccitelli GC, Distefano D, et al. Brain Tumor-enhancement visualization and morphometric assessment: A comparison of MPRAGE, SPACE, and VIBE MRI techniques. *American*

ACCEPTED MANUSCRIPT

Journal of Neuroradiology. **2019;40:1140EP-1148. DOI: https://doi.org/https://dx.doi.org/10.3174/ajnr.A6096**

10. Kim D, Heo YJ, Jeong HW, et al. Usefulness of the delay alternating with nutation for tailored excitation pulse with t1-weighted sampling perfection with application-optimized contrasts using different flip angle evolution in the detection of cerebral metastases: Comparison with MPRAGE. ***American Journal of Neuroradiology.*** **2019;40:1469EP-1475. DOI: https://doi.org/https://dx.doi.org/10.3174/ajnr.A6158**

11. Kongpromsuk S, Pitakvej N, Jittapiromsak N, et al. Detection of brain metastases using alternative magnetic resonance imaging sequences: A comparison between SPACE and VIBE sequences. ***Asian Biomedicine.*** **2020;14:27EP-35. DOI: https://doi.org/https://dx.doi.org/10.1515/abm-2020-0005**

12. Fu Q, Cheng QG, Kong XC, et al. Comparison of contrast-enhanced T1-weighted imaging using DANTE-SPACE, PETRA, and MPRAGE: A clinical evaluation of brain tumors at 3 Tesla. ***Quantitative Imaging in Medicine and Surgery.*** **2022;12:592EP-607. DOI: https://doi.org/https://dx.doi.org/10.21037/qims-21-107**

13. Jun C, Shuhua L, Xue Z, et al. Application of motion-sensitized driven equilibrium based black blood 3D TSE sequence in the detection of brain metastases. ***Magnetic Resonance Imaging.*** **2022;93:145EP-148. DOI: https://doi.org/https://dx.doi.org/10.1016/j.mri.2022.08.010**

14. Gule-Monroe M, Chasen N, Long JP, et al. Diagnostic Confidence of Contrast-Enhanced T1- Weighted MRI for the Detection of Brain Metastases: 3D FSE-vs. 3D GRE-Based Sequences. ***AJNR American journal of neuroradiology.*** **2024. DOI: https://doi.org/https://dx.doi.org/10.3174/ajnr.A8590**

15. Chen Zhou ZH, Salvador Alvarez E, Hilario A, et al. Improved detection of brain metastases using contrast-enhanced 3D black-blood TSE sequences compared to post-contrast 3D T1 GRE: a comparative study on 1.5-T MRI. ***European Radiology.*** **2025:8. DOI: https://doi.org/https://dx.doi.org/10.1007/s00330-025-11363-0**

ACCEPTED MANUSCRIPT